Clogging Mechanisms in Converging Microchannels

Clogging Mechanisms in Converging Microchannels

A dissertation presented
by
Sorell Sumner Massenburg
to
The School of School of Engineering and Applied Sciences

in partial fulfillment of the requirements
for the degree of
Doctor of Philosophy
in the subject of
Applied Physics

Harvard University
Cambridge, Massachusetts
July 2015

Thesis advisor: Professor David A. Weitz Sorell Sumner Massenburg

Clogging Mechanisms in Converging Microchannels

Abstract

Many technological and biomedical applications ranging from water filtration and oil extraction to arteriosclerosis and vein thrombosis rely upon the transport of solids in liquids. Particulate matter suspended in liquid flowing through channels that are often microscopic or millimeters in size which leads to clogging. This dissertation examines the clogging behavior of microscopic channels by microscopic particles suspended in liquid. We physically model clogging in microchannels by flowing microparticles through microfluidic channels. Unlike previous studies, we choose non-uniform microchannels; specifically, we study clogging in microchannels whose width narrows over the length of the channel. Converging channels are inspired by the pore size variations in real porous media like membrane filters and sandstone.

Initially we study the clogging behavior of microparticles in arrays of parallel microchannels as we vary the microchannel entrance (mouth) width and microchannel length. We measure the time until each channel clogs and we calculate the number of particles that pass prior to clogging. Contrary to expectation, we show that the number of particles passing through a pore increases exponentially with increasing mouth width but decreases linearly as the channel length increases. Changing the dimensions of the channels changes the particulate suspension's flow rate which in turn changes the shear stresses that particles experience near the channel wall. When particles experience higher near-wall shear stress, the particles are less likely to adhere to channel walls and engender clogging. We confirm the effect of flow rate on channel clogging by demonstrating that the number of particles needed to clog a tapered channel increases as the pressure applied to the particulate suspension increases.

The connection between flow rate and clogging highlights the interplay between hydrodynamic forces and intermolecular forces that govern particle attachment and ultimately clogging. We further explore this relationship by modulating the interaction between the particle and channel wall in a single tapered channel. While observing single channels clogging, we also resolve individual particles gradually building up on channel walls and forming clogs. Interestingly, particles also cluster on upstream channel walls only to later detach and clog at the downstream constriction. At low

s

pressures, the channel clogs when particles accumulate individually near the constriction. At high pressures, the channel clogs when particle clusters detach from channel walls upstream and flow into the constriction. Finally, we compare the clogging behavior of particles with long, electrosteric stabilizing molecules on the surface to the clogging behavior of particles with shorter electrostatic stabilizing molecules on the surface. We also compare the clogging behavior of both particle types in the presence of varying concentrations of a monovalent salt. We show that clogging is mitigated when Debye length is comparable to the length of the stabilizing molecule on the particle's surface.

Contents

Listing of Figures

Dedicated to:
Howard H. Sumner Sr., Autodidact

Acknowledgments

Following a long Ph.D. trajectory, assembling a thank you list is a task that is almost as Herculean as the dissertation itself. There have been many individuals and institutions that have given me scientific and personal advice, support, funding and inspiration. Certainly, my sieve-like memory has not retained all of their names. I regret that I cannot compile a complete list of my many sources of help. However, my failure reminds me that I am truly fortunate to have had so much help over the years. And those who are fortunate, must give thanks.

I would be remiss if I did not thank David Weitz for allowing me to participate in what I consider to be the largest soft matter projects on the planet: "the self-assembled lab". Specifically, he provided opportunity for many scientists and engineers from all over the world to aggregate in single location: The Experimental Soft Condensed Matter Group. The group contains a large number soft matter experts and budding scientists who are unencumbered by hierarchy and bureaucracy and within the group, knowledge diffuses freely. With a large number of scientists coming and going, the lab seemed like a busy intersection, a major crossroads in the world of soft matter. I have been delighted to rub elbows with colleagues from far flung places. In the process, I have learned a great deal from my laboratory colleagues. Without my colleagues, my work would have progressed at a snail's pace and its quality would have most assuredly suffered.

A number of colleagues contributed to my work and to my growth as a scientist, but none more than Esther Amstad. I will be forever grateful to Esther for her scientific leadership and mentorship just as I am grateful that she serendipitously worked at a desk immediately behind me in the lab office. For a young scientist, watching Esther work was a masterclass in scientific efficiency and professionalism. As she juggled multiple engineering and science projects, Esther set a sterling example for less experienced scientists. I am honored and grateful for her mentorship and support over the past four years. In addition to juggling numerous projects of her own and managing other students, Esther found the time to learn about my project and give me crucial advice and suggestions, much like a Ph.D. adviser. Through her example and direct guidance, she taught me one of the most important skills a scientist can possess: the ability to efficiently design and plan experiments to reveal the most interesting features of an experimental system. I am also thankful for her help in learn-

ing other important skills like scientific writing and collaboration. Even after leaving Harvard and starting her professorship, Esther carved time out of her schedule to advise me via Skype ™. Like a coach encouraging a hurdler on a running track, Esther challenged and inspired me as I encountered obstacles in the final, arduous stretch of my Ph.D. journey.

Early on during my tenure in the Experimental Soft Condensed Matter Group, a knowledgeable and amicable post-doctoral fellow name Jeremy Agresti had an insight about our microfluidic technology. Jeremy observed that nearly all microfluidic devices used in lab would clog if given enough time. Most fellow lab members were content to utilize on-chip filters designed to delay the onset of clogging. Rather than delaying the inevitable, Jeremy saw a unique opportunity to study clogging in microfluidic channels. Although Jeremy proposed this topic as a way to improve microfluidic devices we soon learned that clogging was intimately related to another problem, fouling. Fouling, especially biofouling is a world-wide problem that costs billions of dollars per annum. Given this inspiration, I initially focused on preventing biofouling by studying clogging in microfluidic channels by cells. Cells proved to be a too complicated for initial clogging studies and I chose to use colloids in lieu cells. My choice of colloids proved useful for developing a better, more widely applicable model system.

The colloidal choice was affirmed upon meeting Onur Kas of the Millipore Company (now EMD Millipore). Onur shared with me the importance of clogging in filtration and inspired me to use tapered microchannels to mimic asymmetric membrane filters. I am thankful to Onur Kas for his inspiration and valuable input into my clogging project. His example of an application in which clogging is beneficial helped to convince me that clogging is an occurrence that should be understand and controlled rather than merely prevented. Therefore, I thank Onur Kas for helping transform my study from an engineering project: preventing clogging in microchannels to a scientific project: Clogging Mechanisms in Converging Microchannels. Specifically, I must credit Onur with the idea of studying converging microchannels as an approximation of asymmetric membrane filters.

Many others have informed my experiments. Chiefly, I must thank Wynter Duncanson, the friendlies and liveliest post-doctoral fellow from the Experimental Soft Condensed Matter Group. Like Esther, Wynter provided an excellent scientific example for graduate students and PhDs alike. One of the chief scientific lessons Wynter imparted to was to know when my results were “good enough”. She helped me understand that I didn’t have to boil the metaphorical ocean to do good science. With her I learned when to perform efficient, quick exploratory experiments and when to do more exhaustive yet short and efficient experiments.

A number of individuals have contributed directly to this project. First I must thank Thomas Kodger for particle synthesis and frequent experimental advice. Tom is an excellent chemist and

experimentalist. His wizardry with colloidal chemistry and willingness to share it was a boon to the entire research group, including me. Specifically, Tom was acutely helpful when I needed to tailor the interactions between particles and between particles and channel walls in my experiments. Tom crucially provided the particles used in many of my experiments. Also, Tom showed me how to use polyelectrolytes to coat microfluidic channel walls. In addition to these significant contributions, I am also grateful for the constant experimental advice that Tom provided to me and the entire group. I also thank James Travers, a high school student at the time, for experimental help. James patiently measured the resistance of microfluidic devices that proved quite useful in my experiments on arrayed microchannels. Kaare Jensen was also a significant resource during my experiments. Primarily he was an excellent discussion partner. Our discussions were fruitful and conversing with Kaare provided useful context and helped me place my experiments in context.

Also I am thankful to Lloyd Ung, Donald Aubrecht, Ralph Sperling, Rodrigo Guerra and Emily Russel for experimental help. Lloyd, Don and Ralph provided very helpful experimental mechanical suggestions. I am grateful to have rubbed shoulders with such excellent engineers and experimentalists. Rodrigo took the time to show me how to synthesize polymer particles and even synthesized a batch for me. Although I did not use his particles in my experiments, I learned a great deal from him and I appreciate his willingness to help. Emily Russel also provided valuable experimental help. She was very generous in sharing her particle stocks which proved useful in exploratory experiments.

In addition to the aforementioned individuals, various members of the Experimental Soft Condensed Matter Group were very helpful during my graduate school career. Naveen Sinha was a great colleague, excellent companion and overall good influence. Naveen's dedication and varied interests inspired me and taught me a great deal. I must specifically thank Naveen for introducing me to Genius Hour where we held many productive work sessions and fruitful brainstorming meetings. Helen Wu was also an excellent and cordial colleague. I appreciate her down to earth personality and common sense approach to the laboratory and life in general. I am thankful to Louise Jawerth for constantly asking questions and making suggestions. Her questions were honest, pointed and always shed light into my experiments. Don Aubrecht taught me an important lesson for which I am grateful; always keep an engineer around. Ilke Akartuna and Dorota Koziej were two post-doctoral fellows who always made time to chat with me about life and science and any shared interests. As a visiting student from Germany, Simone Bachtler, was a wonderful colleague who shared tea and scientific ideas with me, taught me a great deal about her native land and even hosted me when I visited her hometown. More than anyone, I credit Simone with sparking my passion to learn the German language. Also Kisun Yoon freely shared his colloidal expertise from the time I was a fledgling undergraduate student in the Manoharan Lab until he left the laboratory.

Additionally, I sincerely thank Oni Basu, Liheng Cai, Adrian Pegararo, Zsolt and Kate Jensen from the Experimental Soft Condensed Matter lab and Spaepen lab for their congenial attitude and helpful scientific input. Although Oni (also known as One and Only Oni) is a biologist, a great one at that, she was never shy about inquiring about my clogging experiments or about giving me helpful suggestions and she was never too busy to talk about science or any of our common interests. Adrian Pegararo is also a fantastic biologist who never hesitated to lend his sharp mind to any experimental or scientific issues that I faced. I appreciated Liheng's chemistry expertise and his useful suggestions. Specifically, I thank him for chemistry knowledge that he provided around 3 am one night as we sat in Dave's office waiting for Dave to awake from a nap. His input was crucial to helping me understand and verify my results in Chapter 3. Colloidal experts Zsolt and Kate split their time between the Experimental Soft Condensed Matter and the Spaepen lab and freely shared their colloidal wisdom and expertise.

Thank you to Vinothan Manoahran and numerous members of his lab. Vinny first hosted me in his lab as an REU student and truly shifted my research interests towards Soft Matter. While in his lab I learned a great deal about colloids, being independent and about persistence. As a graduate student, his lab was a second laboratory home. I frequently ventured across the hall to the Manoharan lab, sometimes purposefully but usually aimlessly. I was always welcomed in the lab and his lab members were immensely helpful. Specifically, Anna (Anner) Wang shared not only my interests in Soft Matter but in food and mixtures as well. It was incredibly fortuitous that we were teaching fellows for science and cooking together. I appreciate her sense of humor, "mateship" and willingness to entertain my rambling ideas about science and life in general. Additionally, from the Manoharan lab, Guagnon Meng was an excellent REU mentor and was a great asset during my Phd. Studies. Sofia Magkiriadou was a wonderful class mate (Statistical Thermodynamics) and hallmate (Conant 4^{th}) during our first year at Harvard. She continued to be a resource while in the Manoharan lab. I am thankful to David Kaz for his experimental wizardry and to Ryan McGorty, Viva Horowitz, Tom Dimiduk and Becca Perry for their constant help and welcoming attitude.

From SEAS and Physics, I would like to thank Kathryn Hollar and Melissa Franklin. When I was an undergraduate, Kathryn sought me out at the National Society of Black and Hispanic Physicists Conference. Her friendly disposition convinced me that not everyone at Harvard was pretentious and that I should apply for the REU program. I am thankful that she convinced me to apply and join Harvard's REU program. I am grateful to Mellissa Franklin for her constant support for students in the physics department and even students like me who were not in the physics department. A consummate professor, Melissa shows genuine concern for the development of students in physics at both the undergraduate and graduate levels.

I am imminently grateful to my HMSG colleagues and friends. Many thanks to Prof. Peter Blair for his inspiring example, continued encouragement and motivation and constant willingness to hash out scientific ideas. Additionally, Rafael Luna proved to be a great resource and an uplifting friend. I am grateful for his attention to my manuscripts and his willingness to teach me "Scientific Storytelling". Martin Mwangi, Renita Horton, Deriba Olana and James Whitfield all deserve thanks for being scientific colleagues and encouraging friends.

For funding my PhD, I am grateful to the Ford Foundation for awarding me their pre-doctoral fellowship and allowing me to participate in an incredible community of scholars. Also, I am sincerely thankful to Harvard GSAS, Harvard SEAS and the NSF MRSEC for making my scientific journey financially viable.

I am grateful to Lino Pertile for inviting me to be a tutor at Eliot House. I am very grateful to Doug Melton and Gail O'Keefe for keeping me on at Eliot House and helping make the Eliot Community a home. I am also grateful to Eliot House for the opportunity to serve as acting dean to House for a semester. I am dumbfounded that you placed your trust in me and I am ever grateful for the experience. To Mahi M., thank you for the Chai Chats and interrupting my work in helpful ways. To Eliot House as a whole, I am grateful to have participated in such a wonderful and dynamic community during my scientific journey.

I would like to thank Prof. Andrew Richardson for envisioning and hosting the class on scientific writing, OEB 210. In this class, I learned how to think of myself not just as a scientist but as a writer and communicator. I will ever be grateful the ideas and acronyms that I learned in this class like "schemas', OCAR and story arcs. Additionally, I am grateful to the teaching fellow, Jon Sanders, and my peers for allowing a non-biologist into their group and helping me learn to think critically about written scientific communication.

Jordan Suchow, I am grateful to you for making your dissertation template freely available. You save me countless hours. To typeset this dissertation, I used his LATEX template freely available at: https://github.com/suchow/. To Michael Adrian Davis, thank you for leading the Early Morning Praise Party on the radio each weekday morning. That radio program was the perfect soundtrack to many dreary mornings when I needed to arise before the sun.

Last and farthest from least, I thank Nedra Massenburg for her patience. I am grateful not just for her patience through a long Ph.D. process but that she listens each time I stop explain a random physics concept that I notice in action in our midst. Nedra tolerated my late night meetings with Dave and all night experiment sessions with minimal complaint. I also thank Sorell & Joyce Massenburg for my name, my birth and never-ending support. I am thankful that they gave me a long enough leash to find my own way in life. To Howard & Mary Sumner and Jeremiah & Doris

Sumner, thank you for helping raise me and for your continual support. Specifically, I am deeply grateful to the late Howard Sumner for his autodidactic example; it has a been a constant source of needed inspiration during my Ph.D. journey. While living, he frequently encouraged me to "get all the education that you can get". I hope that my Ph.D. is a good start towards such a lifelong goal. I must also thank Edith Battle for *gently* threatening me when I expressed reluctance to go to Harvard. Finally I am grateful to Van Battle for helping push me over the finish line with seven words of wisdom: *the best dissertation is a finished dissertation*.

Thoroughly conscious ignorance is the prelude to every real advance in science.

James Clerk Maxwell

1

Introduction

The transport of solids suspended in liquids through conduits impacts a large number of commercial and scientific applications. Occasionally these solids become trapped, and accumulate in the conduit and severely restrict fluid flow; this condition will be referred to as clogging. In the simplest case, size exclusion causes clogging when suspended particles attempt to flow through conduits whose diameter is smaller than the particle size. Even when the particles are much smaller than the size of conduit, clogging can occur when particles successively adhere to the conduit walls and impede fluid flow. This clogging process is present in a variety of situations, ranging from biological settings like heart disease to industrial settings like oil extraction.

Crude oil, extracted from underground reservoirs, is often pumped through porous rock at high pressure. Pores in the rock frequently clog due to the solids contained in the crude oil.[1] As more

crude oil flows through the porous rock, more pores clog which limits the extraction of the valuable crude oil. While clogging is an expensive problem in oil extraction, it can be lethal in plants and animals. In leafy plants and trees, for example, bacteria and fungi can lodge in the xylem. Accumulated bacteria or fungi in the xylem can choke the flow of nutrient laden water through the plant.[31] With their xylem clogged, these plants slowly wilt and die, leading to crop failure or disruptions in the natural habitat. Clogging in humans, can also be deadly. Substances like cholesterol and fatty plaques deposit and buildup in arteries, impede blood flow and contribute to heart attacks and strokes.[24,26] Given the destructive nature of clogging in these instances, industrial engineers and medical scientists have worked intently, but unsuccessfully to eliminate arterial clogging.[31,3]

Instead of viewing clogging as destructive, filtration companies view clogging as a vital feature.[4] Filters are designed to remove harmful solids like dirt and bacteria from soiled fluids in order to clean and sanitize it. Because clogging is essential to filtration function, filtration companies strive to enhance and optimize clogging in membrane filters – rather than eliminate clogging altogether. Minimizing bacterial wilt in crops, fouling in oil wells and atherosclerosis while enhancing clogging in filter membranes, requires a deep scientific understanding of clogging; rather than a concerted engineering effort to eliminate clogging. For decades, there have been attempts to understand the nature of clogging, with varying degrees of success.

1.1 Early Work on Clogging Mechanisms

Clogging mechanisms have been studied in the context of filtration since the 1930's[13]. Four processes were envisioned: complete blocking, standard blocking, intermediate blocking and cake filtration. In complete blocking, size exclusion prevents particulates from entering the pores. Standard blocking occurs when particles smaller than size of the pore stick in the interior of the pore and eventually block it. Intermediate blocking results from particles that block at the entrance but can also reside in the space between pores and therefore has a lower probability of blocking than in the complete

blocking case. Finally, cake filtration occurs when the particles are significantly larger than the pore and multiple layers of particles deposit on top of the pore surface.

Using Darcy's law and assuming a flow driven by a constant pressure source, it was found that each process follows the same power law, but with a different exponent, n:

$$\frac{d^2t}{dV^2} = k\left(\frac{dt}{dV}\right)^n \tag{1.1}$$

The complete blocking mechanism fulfills the power law with an exponent of two. The exponent for standard blocking is 1.5. In the case of Intermediate blocking, the power law has an exponent of one and in the case of cake filtration the exponent is zero. This power law successfully connected unobserved clogging mechanisms with the two primary measurable components of filtration: time and volume passed through the filter. These laws were later expanded to include non-Newtonian fluids.[17] The Newtonian and non-Newtonian versions of the power laws continue to be used in scientific and industrial settings[14,22,27,19,28]. These blocking laws represented a significant leap forward in the 1930's and enable clogging mechanisms to be detected in in membranes. However, the utility of these laws largely resides in detection, not comprehension. The power laws offer little to help in understanding the physical nature of clogging mechanisms. Additionally, the power laws do not cover all clogging mechanisms and their application is usually confined to membranes.

1.2 Challenges in Studying Clogging

Understanding the mechanisms that control individual pore clogging is challenging without imaging the clog formations. In situ, real time imaging of clogging in arteries and plant xylem is not yet practical. Although computerized axial tomography of porous rock is often used to study multiphase flow in porous rock[29], CT scans have yet to provide high spatial resolution and high temporal resolution at reasonable cost. These difficulties can be circumvented with a micro model that en-

ables clog formation to be imaged. In addition to imaging, the microchannel model system should feature the ability to alter the interactions that lead to clogging.

The interactions that occur between a particle and a wall or between two particles are usually categorized as intermolecular forces[15] and are effective at lengths scales that range from nanometers to a few micrometers. Therefore, a micromodel must be a small enough to allow intermolecular forces to influence the system while remaining large enough to be visualized using optical microscopy. Additionally, the applications of clogging feature a wide range of interactions between the constituent particles and pores and channels. For example, intermolecular forces experienced by particles in crude oil flowing through porous rock are different from the intermolecular forces experienced by bacteria in plant xylem. A relevant micromodel will enable the examination of these differences by permitting the modification of the interactions between two particles or particles and the wall.

Like intermolecular forces, the hydrodynamic forces differ in various different real-world scenarios. For example, the fluid dynamics of a suspension flowing through porous rock is very different from a suspension flowing through a plant xylem. Again, a widely applicable micromodel will allow the researcher to control the fluid behavior by modulating the size and shape of the microchannel as well as the flow through the channels. As our micromodel is intended to clog, we anticipate the need to use a new micromodel for each experiment. Accordingly, we impose a final condition: the micromodel should be disposable. Thus we require the micromodel to be inexpensive and easy to replicate. Even though we impose a variety of strong requirements, we find a system that meets them.

A combination of (poly) dimethyl-siloxane (PDMS) microfluidic channels and colloidal particles suspended in fluid comports with our imaging, force control, hydrodynamic customization and disposability requirements. PDMS microfluidic channels can be made by polymerizing inexpensive PDMS elastomer and coatings can be applied to the channel walls. Each mold is easily reused more than 100 times and can be made in a wide of range of sizes and in any 2 dimensional shape using soft

lithography techniques.[5] Colloidal science also offers cost effective methods to fabricate monodisperse polymer particles while controlling their size and surface functionalization.[5]

1.3 Microfluidic Clogging Studies

Since the 1990's, engineers have utilized microfluidic technology to engineer solutions to biomedical and industrial problems while scientists have exploited microfluidics as a platform to study science at the microscale. Microfluidics has been used to study clogging since the early 2000's. In 2006, researchers clogged arrays of 30 parallel PDMS microchannels by flowing latex particles suspended in water through the channels.[30] The particle size was always smaller than the channel size even though the ratio of microchannel size to particle size varied by an order of magnitude. The particles were stabilized with carboxyl groups and spontaneously attached to the PDMS surface and eventually clogged the channels. The average time to clog an array of microchannels was halved when the applied pressure was doubled and the particle size and channel size were held constant. * The inverse proportionality between clogging time and applied pressure implied that a constant volume of suspension must pass through the channels prior to clogging. A constant volume passed prior to clogging indicates that a constant number of particles also passed before clogging and therefore the number of particles passing through a pore determines whether a channel will clog. The number of particles needed to clog microchannels increased with channel size and particle size. Additionally, the time to clog decreased with increasing salt.

Another study tested the clogging behavior of polydisperse particle suspensions in large arrays of microchannels shaped identically to the microchannels tested in the previous study.[20] Even a small number of particles that were large compared to the mean particle size dramatically altered the time to clog a microchannel. These observations showed that the mean particle sizes of polydisperse sus-

*However, the authors only reported the average time using two relatively high applied pressures (2 PSI and 4 PSI

pensions are poor estimators of clogging time and the degree of polydispersity influences whether microchannels are likely to clog by the buildup of multiple particles or size exclusion.

The aforementioned qualitative findings were later confirmed quantitatively in another study[23] that also utilized microchannels with a shape similar to the previously published experiments. This more quantitative study showed that the interval between clogging events in large microchannel arrays followed the Poisson distribution and that the mean interval between clogging events varies inversely with the relative concentration of large "contaminants". Using the relationship between mean clogging interval and contaminant concentration, the clogging behavior of microchannels can be leveraged to measure contaminant concentration in particulate suspensions.

The microfluidic experiments show that flowing colloidal suspensions through microfluidic channels can provide broad insights into the process of obstructing flow through channels by accumulating particles on the channel walls. Wyss et al.'s[30] experiments illuminate the physics of clogging by providing an elegant scaling law. Instead, Stoeber et al. and Sauret et al.'s insights are more applied and suggest a novel use for clogging in microchannels.[20,23] However, the three aforementioned experiments are limited in two important ways: channel geometry and clogging mechanisms. Each microfluidic study used similarly shaped channels in arrays of 20-40 channels as shown in Figure 1.2. Additionally, each series of experiments only considered clogging to result from the blockage of single particles whose size is approximately the size of the channel or clogging resulting from the buildup of particles that are smaller than the channel.

Another study eschewed the common channel shape and compared straight microchannels to a network of microporous channels that were connected and/or staggered.[2] The authors, observing the channels as an aggregate, found that the connected channels retained the most particles in the network interior while the straight channels prevented the most particles from ever entering the channel network. The authors observed similar behaviors at even when the fluid speed increased. In relation to filtration, the authors found that connected and staggered (tortuous) channel networks

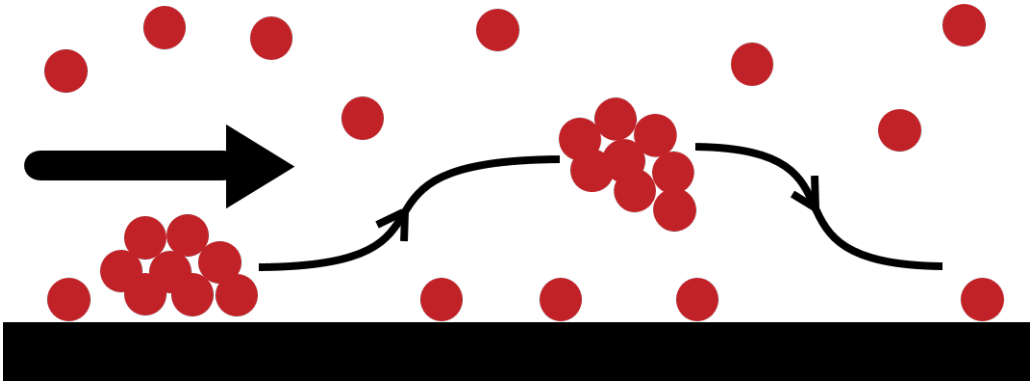

Figure 1.1: Illustration of a cluster of particles detaching from a surface and redepositing downstream.

showed the highest capture efficiency. These experiments provided a significant step away from the more frequently used microchannels with uniformly varying width. However, this study was limited by channels by a common, unchanging channel width and by observing the channels in aggregate rather than individually.

1.3.1 Other Microfluidic Studies

Additional clogging mechanisms, such as particle and cluster detachment and re-entrainment, are thought[9,12] to induce clogging but not well studied. In cluster detachment, flowing particles that are smaller than the channel width aggregate into clusters on pore wall that are similar in size to the channel through which they flow. The cluster grows as more particles attach to it and eventually detaches from the wall and re-entrains in the fluid. Microfluidic channels and colloids also provide a convenient system to study cluster growth and resuspension.

Microchannels have also been used to observe cluster formation on channel walls by particles flowed at a constant volume[10]. Electrically neutral, sterically stabilized microparticles were flowed through rectangular PDMS microchannels. The particle size and channel height were similar to the particle size and the microchannel height used in previous microchannel clogging experiments. However, in

these experiments, the length and width of these channel were more than one order of magnitude larger the microchannels used in microchannel clogging studies. Instead of clogging the wide channels, the particles successively adhered to channel walls and formed clusters. The area of a surface-bound particle cluster was found to grow linearly over time. The total cluster area increases with particle volume fraction increase and increasing the particle size increases the number of clusters while maintaining a constant cluster area. Interestingly, the particle clusters tended to merge and break apart in response to flow-induced stress. Although observation of cluster formation and detachment hints that particle clusters can form and detach in microchannels, cluster induced clogging has yet to be directly observed.

1.4 Structure of the Dissertation

This dissertation presents two projects that look for new insights into clogging microchannels by altering experimental parameters that were overlooked in previous studies.

In Chapter 2, we examine the effect of altering microchannel geometry. One of the biggest advantages of using microfluidic channels is two dimensional spatial control. The size and shape of microchannels are easily varied over a range of scales. Yet, most previous microfluidic studies of clogging focused on clogging in channels whose channel width varies periodically along the length of the channel as seen in Figure 1.1. While this periodically varying width channel geometry provided an effective shape for clogging, re-using this shape neglects an experimental parameter than is both easy to manipulate and likely plays an important role in clogging.

Changing the shape and size of the microchannels strongly affects the flow profile and hydrodynamic forces of the fluid flowing through the channels. Altering the hydrodynamic forces should strongly affect clogging because clogging results from competition and cooperation between hydrodynamic and intermolecular forces. Instead of channels with periodically varying width, we use channels whose width decreases along the length of the channel, or converges. Converging mi-

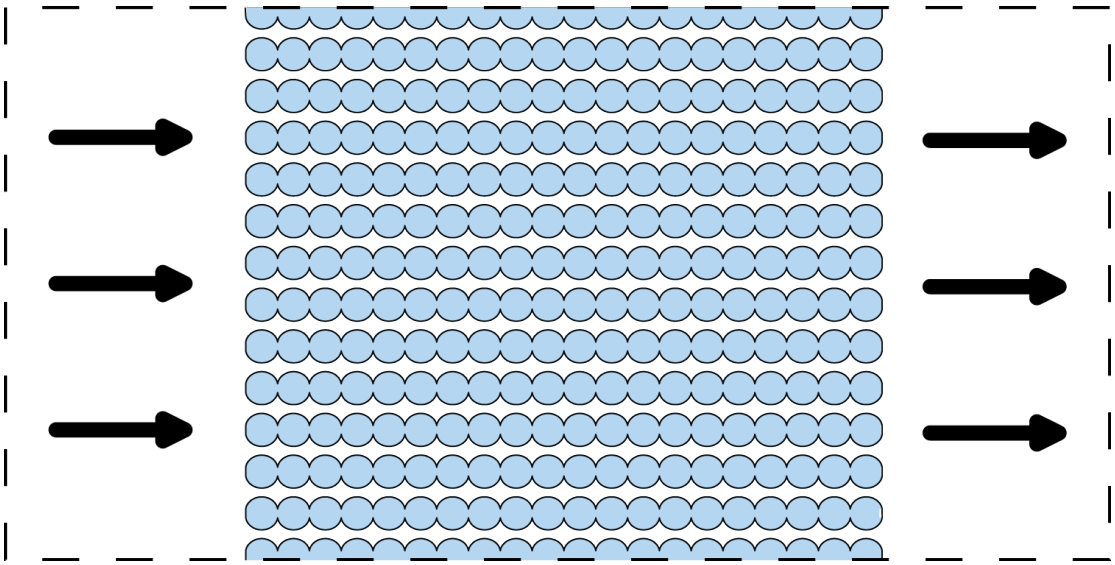

Figure 1.2: Illustrationof array of channels with periodically varying width. These channels are similar to the channels used in published clogging experiments. [30,20,23]

crochannels reflect the properties of real porous materials. Porous media often have a distribution of pore sizes which are sometimes organized into a gradient. In particular, membrane filters are often designed to be "asymmetric" where the pores at membrane entrance are larger than the pores near the membrane exit as shown in Figure 1.3. Membrane filters are designed with asymmetry because asymmetry enhances filtration efficiency for reasons that are not completely understood. [Kas]

In our experiments, we alter the convergence rate of microchannels in 10 channel arrays by varying the mouth (entrance) width of the channel while keeping the throat (exit) width constant. We clog these channels using particle suspensions that are driven by pressure and we vary the particle size. We measure the time needed to clog the channels. Using clogging time and other measurements, we calculate the number of particles that pass through the channels prior to clogging with two methods. Additionally, we vary the pore length and flow rate through the channel for a constant convergence rate and compare the number of particles that pass before clogging. Our observations in Chapter 2 clearly show that flow rate is an important factor in clogging and also suggests that the

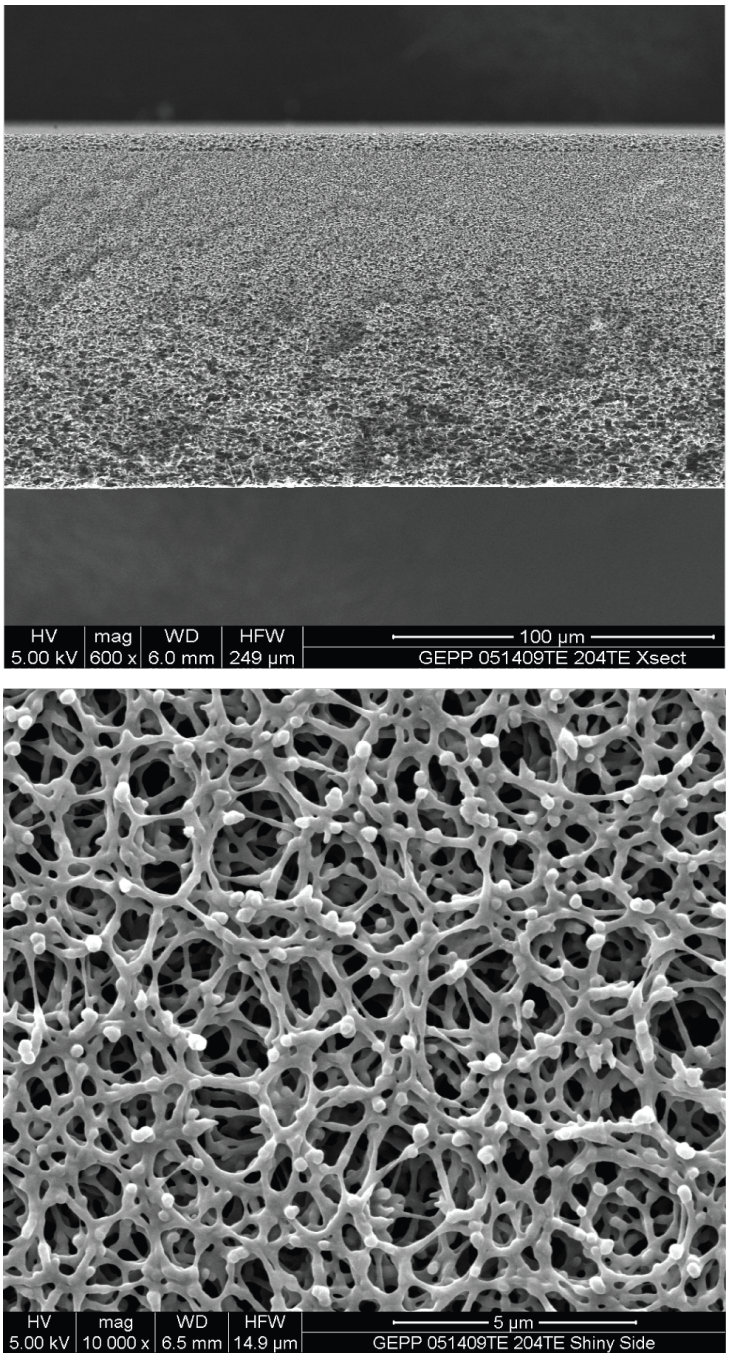

Figure 1.3: Top: Scanning electron microscope image of a polymer membrane filter cross section showing a gradient in pore size. Pores are indicated by the dark areas dispersed among lighter areas. The dark areas increase in size from the top to bottom indicating increasing pore size. Bottom: Scanning electron microscope image of the bottom surface of the (large pore area) of the membrane filter. Image courtesy of Dr. Onur Kas (EMD Millipore).

interaction between particles and the channel walls is also a feature that requires study.

In Chapter 3, we continue varying the flow rate through converging microchannels. In contrast to previous experiments, we examine the clogging behavior of single microchannels instead of ten channels in parallel. We also probe the aforementioned competition between hydrodynamic and intermolecular forces using a different approach. In another departure from previous projects, we exert control over the interaction between the surface and particles. We control the interaction by coating the channel walls with charged molecules and by changing the stabilization of the particles. We further modulate the particle-particle and particle-wall interaction by dissolving salt into the particulate suspension.

An approximate answer to the right question is worth a great deal more than a precise answer to the wrong question.

John Tukey

2

Clogging in Arrays of Tapered Microchannels

In our first project we consider the effect of geometry and flow rate on clogging behavior in tapered microchannels. Principally, we seek to address the question of whether changing a channel's entrance width, while keeping the constriction width constant, will affect clogging in the channel.

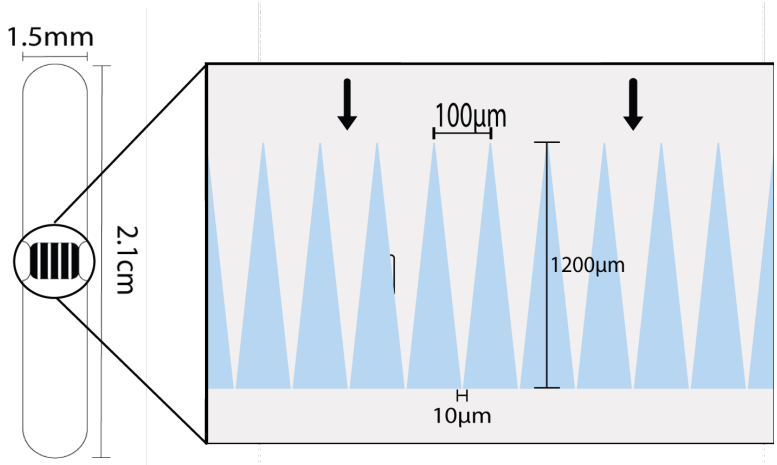

Figure 2.1: Outline of a microfluidic device with an array of 10 channels converging from a mouth width of 100 μm to a constriction width of 10 μm over a length 1200 μm.

2.1 Experimental Methods

To create microchannels, we utilize standard soft lithography techniques that first require drawing and printing photolithographic masks. Using CAD software (Autodesk 2004/2012) we create 2 dimensional drawings of 10 converging microchannels arranged in parallel as shown in Figure 2.1. The mouth (opening) width of the microchannels varies between 20μm and 100 μm while the throat (constriction) width is always 10μm. We vary the length of the microhannel arrays between 300μ m and 1200μm. The microchannel arrays are connected to 1.5 mm diameter round inlet and outlet areas as shown in Figure 2.1. The 2 dimensional drawings are printed by CAD/Art Services, INC (Bend Oregon) on Mylar in the negative at a resolution of 10μm.*

The masks are then used to create molds in photoresist (epoxy) that is sensitive to ultraviolet light.

*For higher resolution we use: FineLine Imaging (Colorado Springs, CO) to print photolithographic masks with 8 µm resolution. For an even higher resolution Heidelberg μPG 501 (Heidelberg, Germany) to write chrome masks with 1 μm resolution.

We spin SU-8 2025/3025 (Microchem, Newton, MA) photoresist onto previously cleaned test-grade silicon wafers (University Wafer, Boston MA). Using a Spincoat G3p-8 spincoater (SCS Coatings, Indianapolis, Indiana) the wafers are spun at 3000 rpm to coat the wafer with a 25μm thick layer of resist. The resist covered wafer is pre-baked on a hot plate (VWR) at 65^{o}C and then at 95^o C [†] and then allowed to cool. The wafer is then covered with the photolithographic mask and exposed to 150-170 $\frac{mJ}{cm^2}$ of ultraviolet light (OAI San Jose, CA). After exposure the wafer the wafer is baked on a hot plate for 1 minute at 65^{o}C and 5.5 minutes at 95^{o}C. It is then developed in propylene glycol monomethyl ether acetate (Sigma Aldrich) and washed with isopropanol alcohol (Sigma Aldrich). After placing in a plastic 100 mm diameter petri dish, the wafer is covered with liquid (poly) dimethylsiloxane elastomer mixed at a 10:1 ratio with curing agent (Dow Corning). The petri dish is baked at 65^{o}C for at least 1 hour. Then the PDMS is cut and peeled from the wafer and 1.2 mm inlet and outlet holes are punched using a biopsy punch (Harris Uni-Core). The punched PDMS chips are thoroughly cleaned and dried using isopropanol alcohol and compressed air. Then, the chips adhered to a substrate using a soft-bake method[6].

In the soft-bake method, a 20:1 PDMS elastomer to curing agent mixture is spun at 100 rpm onto a pre-cleaned glass slide. The glass slide is allowed to bake for 30 minutes at 65^{o}C until the PDMS is soft and tacky. The punched PDMS chip is then placed onto the soft-baked PDMS-slide and the combination is baked at 65^{o}C for at least 30 min. The soft bake method ensures that the channels have a consistent PDMS surface which ensures the particle experiences a constant surface interaction. Other adhesions methods like oxygen plasma exposure cause temporary changes to one surface of the microchannels which may confound experimental results[25].

The microfluidic channels' 1.2 mm inlet holes allow 1/16th (outer diameter) polytetrafluoroethylene (PTFE) tubing (Idex Health & Science Middleborough, MA) to form a tight seal to transport particulate solution from the reservoir. The section of PTFE tubing leading from the microchannels

[†] For SU-8 3025 resist the initial 650C bake is not required.

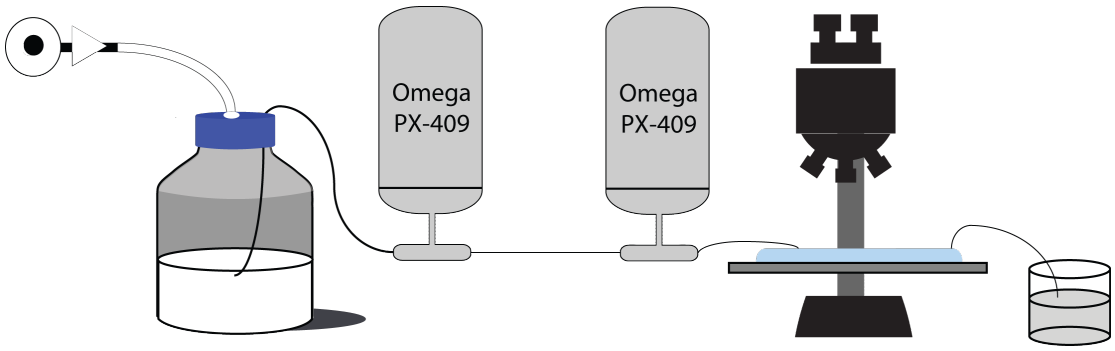

Figure 2.2: Schematic drawing of experimental apparatus. Compressed air pressurizes a glass bottle containing particulate suspension. After the bottle pressurizes, the suspension flows into the submerged tubing and out of the bottle. Continuing to flow through tubing, the suspension flows through a section of calibration tubing located between two pressure transducers (PX). The suspension then flows through the array of microchannels that are watched by a microscope and eventually flow out into a waste beaker.

has an inner diameter of 0.30 inch and connects the microchannel to a T-junction thats joins to a pressure transducer (PX409 Omega, Bridgeport, NJ) and a portion of the PTFE tubing that is used to monitor flow rate.

Using the real time measurements of the pressure difference across a length of tubing with a known resistance enables the approximation of the flow rate of the particle solution in real time even though the particulate suspension is flowed using pressure driven flow.

The tubing used to measure flow rate also has a $1/16^{th}$ inch outer diameter, has a 0.023 inch inner diameter and connects to another pressure transducers. Connecting the 25 cm length tubing to two pressures transducers allows the pressure difference across the length of tubing to be measured in real time. Using the pressure difference (Δp) and the hydraulic resistance (R), if known, the flow rate (Q) can be calculated using the simple formula: $Q = \Delta p/R$. To determine tubing resistance, we flow water (MilliQ) through the length of tubing at varying flow rates using a syringe pump (Harvard Apparatus, Holliston, MA) while measuring the pressure decrease across the tubing. The slope of the line created by plotting ∂P vs. Q reveals the tubing's hydraulic resistance as shown in Figure 5. The measured resistance is typically less than: $10^{-3}\frac{PSI}{L/min}$ which matches the hydraulic

resistance expected from the Hagen-Poisuille equation:

$$\frac{\Delta p}{Q} = \frac{8\mu L}{\pi r^4} \tag{2.1}$$

Using measurements of the pressure difference across a length of tubing during the clogging experiment enables us to approximate the flow rate of the particle solution in throughout the experiment even though the particulate suspension is flowed using pressure driven flow. Once the flow rate is known, the particle flux is estimated by multiplying the flow rate with the suspension's number density. For example, $3\mu m$ diameter particles suspended in water a volume fraction of 4% has a number density 2.83×10^9 particles/mL.

We can also estimate the number of particles that pass a channel before clogging in another way: using the measured clogging time of each channel and the hydrodynamic resistance of a channel. Similar to the calibration tubing, we measure the hydrodynamic resistance of each channel array using a syringe pump and pressure transducers Figure 2.2. We use this method to measure the resistance of the microfluidic device for each unique channel geometry. The resistance of the channel array is much larger than the other parts of the microfluidic device and we therefore consider the resistance of the microfluidic device as the approximate resistance of the microchannel array. Since our ten identical channels reside in parallel to one another, each channel's resistance is ten times the resistance of the ten channel array. After estimating the resistance of an individual channel using our measurements, we compare our estimates to a calculated resistance. We calculate an approximate resistance using Equation 2.2 for the flow rate of a fluid with viscosity mu, driven through a rectangular channel of width, w, height, h, length, L, and by a pressure difference, Δp.

$$\frac{\Delta p}{Q} = \frac{12\mu L}{wh^3}\left(1 - \frac{6(2^5)}{\pi^5}\frac{h}{w}\right) \tag{2.2}$$

Our measured estimates comport well with our calculations.

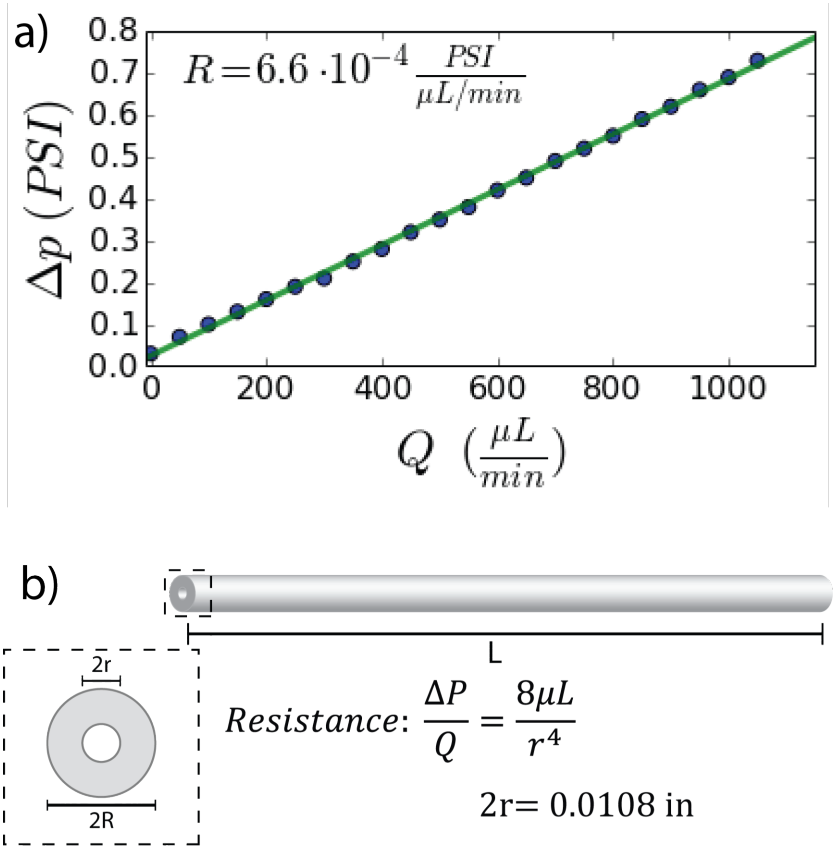

Figure 2.3: (a) A graph of Pressure Difference vs. Flow rate for 50 cm length of calibration tubing where the slope gives the resistance of the calibration tubing. The resistance will later be used to provide an estimate of the flow rate through the channels. (b) A diagram of the calibration tubing showing the inner diameter and outer diameter and the length. The resistance can be expressed as a function of the viscosity, length and inner diameter. Instead of re-calculating the resistance, we use Equation 2.1 to estimate the inner diameter of the tubing to be 0.108 inches. This estimate agrees manufacturer's diameter estimate, and indicates that the resistance measure is accurate.

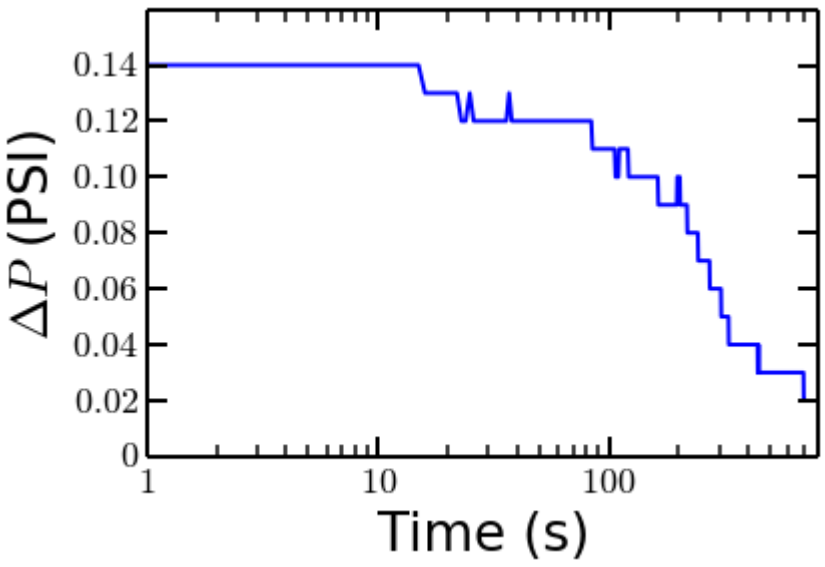

Figure 2.4: A sample pressure trace showing the pressure difference across calibration tubing during a clogging experiment. The pressure trace will be used with the measured tubing resistance to estimate the flow rate during the experiment.

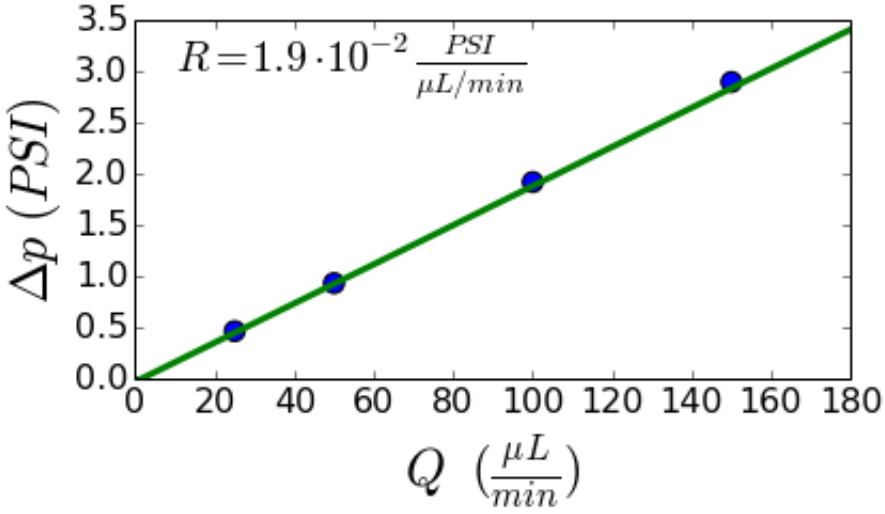

Figure 2.5: A graph showing Pressure Difference vs. Flow Rate measurements for a microfluidic device containing an array of 10 channels. The width of each channel decreases from $80\mu m$ to 10μ over a length of $1200\mu m$.

To calculate the number of particles that pass through a channel before clogging, we first assume that each channel experiences a total flow rate of $Q = \Delta P / R_{channel}$ until the moment it clogs. We use the measured elapsed time before clogging to calculate the total flow through the channel before clogging and then we calculate the number of particles passed before clogging by using the number density of particles in the suspension. We then compare the two estimates and find that they agree within 50

To flow the particulate suspension, we enclose it in an airtight Pyrex bottle (IDEX Health & Science Middleborough, MA). The bottle cap (IDEX Health & Science Middleborough, MA) contains a tapered Luer hole for air supply and a 1/16th inch opening though which tubing can be passed. Tubing that has an 0.030 inch inner diameter PTFE passes through the bottle top and submerges in the enclosed particulate suspension. Particulate solution flows through the when the bottle is pressurized (between 0.5 and 4.0 PSI). The pressure is supplied by 100 PSI house source that is then regulated (Omega) and measured (SSI Technologies). All components of the system are kept at the same height to prevent gravity from affecting the flowrate. Pressure is used to drive the particulate suspension because pressure driven flow ensures changes in flow rate in one channel does not affect the other channels.

The particulate suspensions consist of polystyrene latex microspheres (IDC/ Invitrogen, Woburn, MA) suspended in 37%/63% Water-Deuterium Oxide (D_2O) mixture (Western Analytical Products, (Wildomar, CA). The H_2O-D_2O has a density of 1.04 g/cm^3 which closely matches the suspended microspheres and hinders the microspheres from settling during the course of the experiment. The microspheres are suspended at a volume fraction of 4% (w/v) and are electrostatically stabilized with carboxyl groups. We use particles that are 1 μm, 2 μm or 3 μm in diameter and each suspension is largely monodisperse with a typical coefficient of variation of 0.008. We observe the particulate suspension flowing through the microchannel arrays using optical microscopy (Navitar) and digitally record video at 1 fps (Sony). After exiting the microchannels the particulate suspension flows

through exit tubing into a waste collection that is held at atmospheric pressure.

2.2 Results and Discussions

We first analyze clogging in arrays of 10 microchannels with varying mouth width when the suspension is flowed using an applied pressure of 14 kPa. In the recorded video and resulting micrographs, flowing particles appear as gray, PDMS and liquid absent particles appear white or light and packs of particles appear as very dark or black. A channel is defined as clogged when the stream of particles flowing into the channel is retained somewhere in the channel and no particles can exit the channel. Clogs are identifiable by a sudden appearance of a light region (liquid) just below a very dark region (particle packing) as seen in Figure 2.6.

Using recorded video (Sony, Tokyo, Japan) we measure the time elapsed until each channel clogs. The shape of the fraction of channels clogged vs. time plot is similar for each mouth opening as seen in Figure 2.7. However, the magnitude of clogging time increases as the mouth widths of each channel increases. There is less than order of magnitude difference in the average clogging time for the first clogged channel in a 20 μm-10 μm channel array and the first clogged channel in a 100 μm-10 μm channel array. There is more than an order of magnitude difference in the time to clog the final channel of the two channel arrays.

We also analyze the measured clogging times to detect preferential clogging among the 10 channel array, or whether some channels in the array are more likely to clog than others. For example, if one channel position frequently clogged first among all channels, our channel array would exhibit spatial bias in clogging. If channels in our array are more susceptible to clogging based on their spatial location in the array, then our experiments would probe the effect of array geometry instead of channel geometry.

To test for the spatially biased clogging in our arrays, we assign each channel a value between one

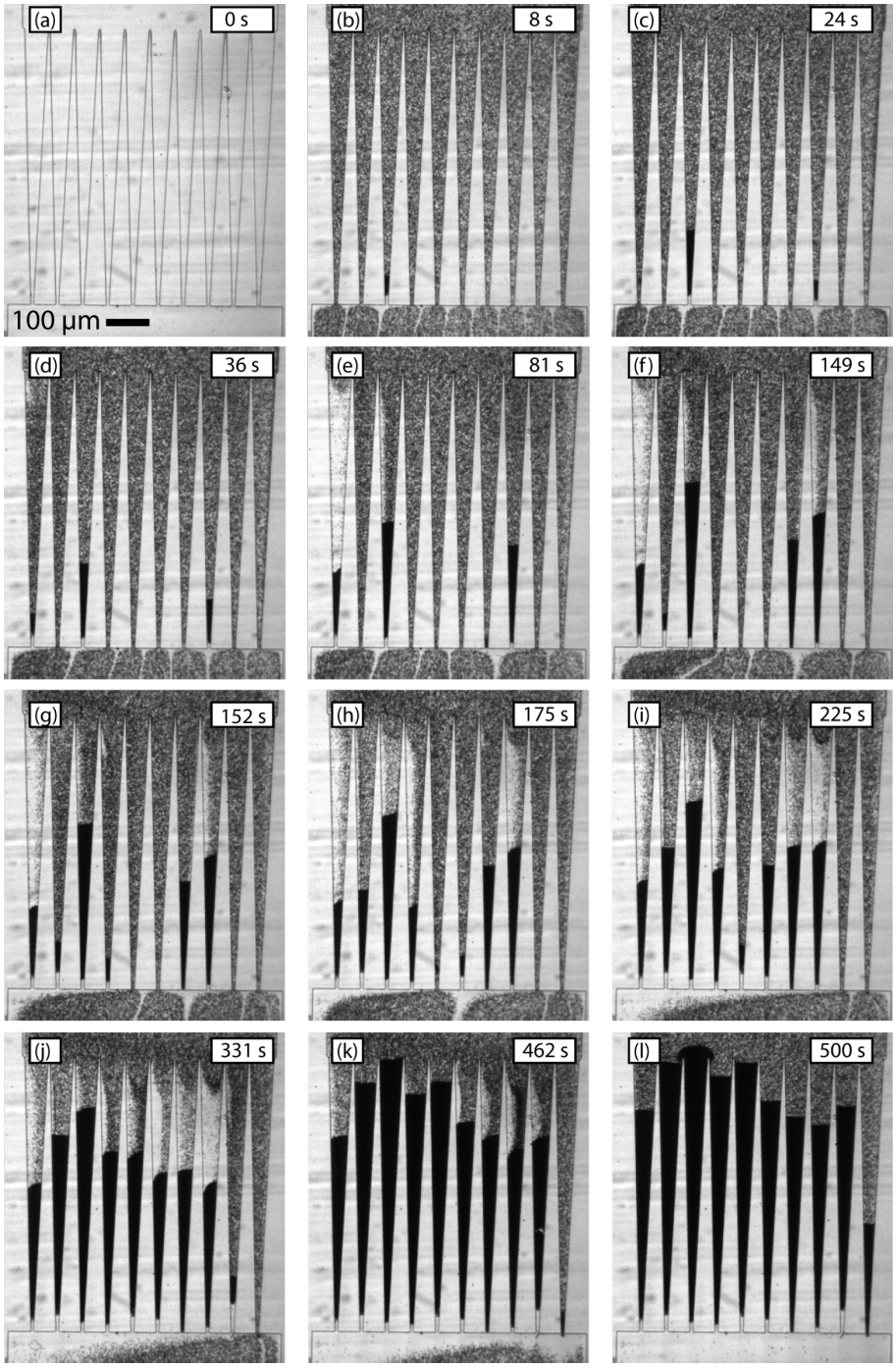

Figure 2.6: (a)Microscopic image of an array of channels clogging. (a) Array just before suspension flows through channel. (b)-(k) Images of the channel array recorded immediately after each channel clogs. (l) Image 38 s after final channel clogs.

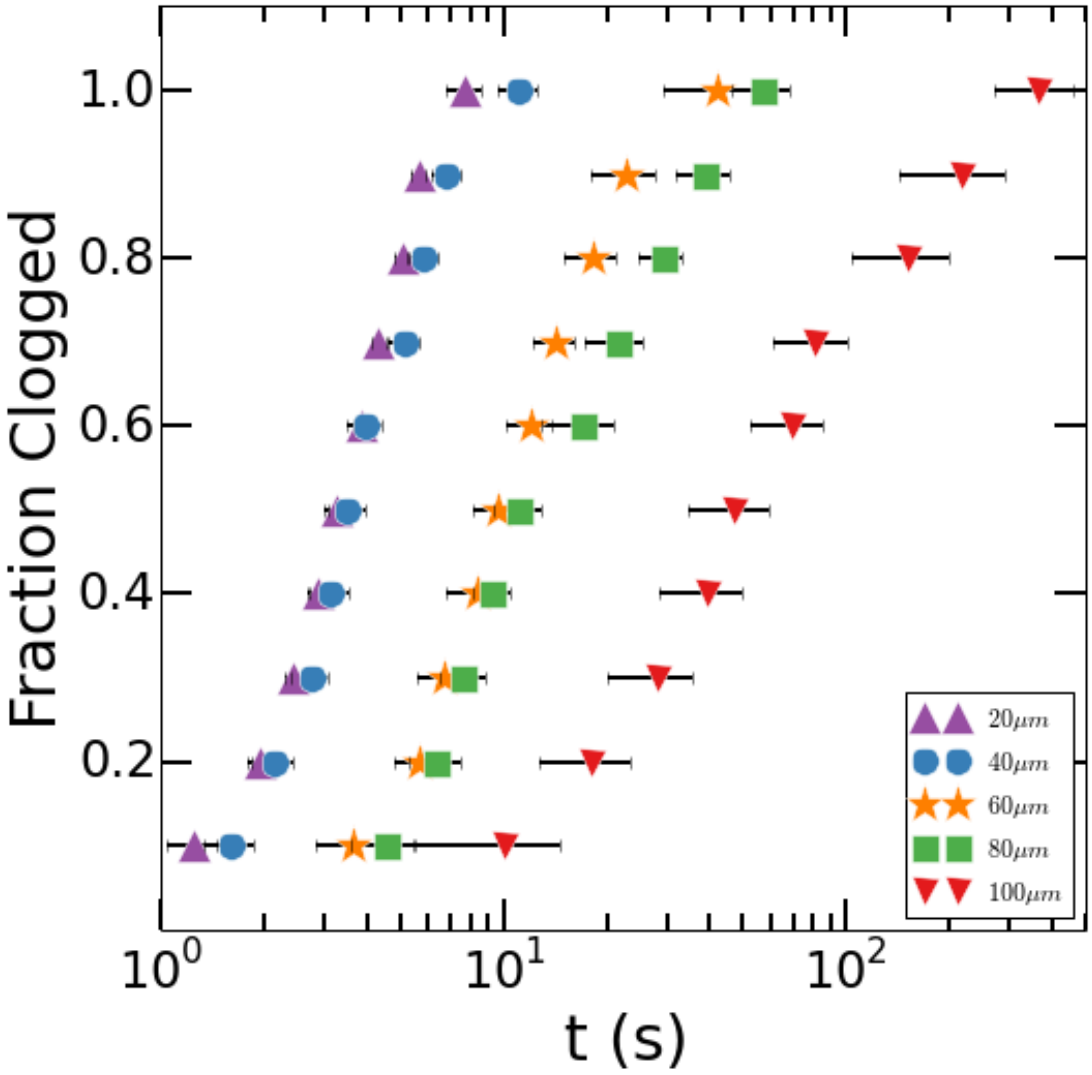

Figure 2.7: A graph showing Fraction of Channels Clogged vs Average Time until clogging for arrays of channels with mouth widths varying from $20\mu m$ to $100\mu m$.

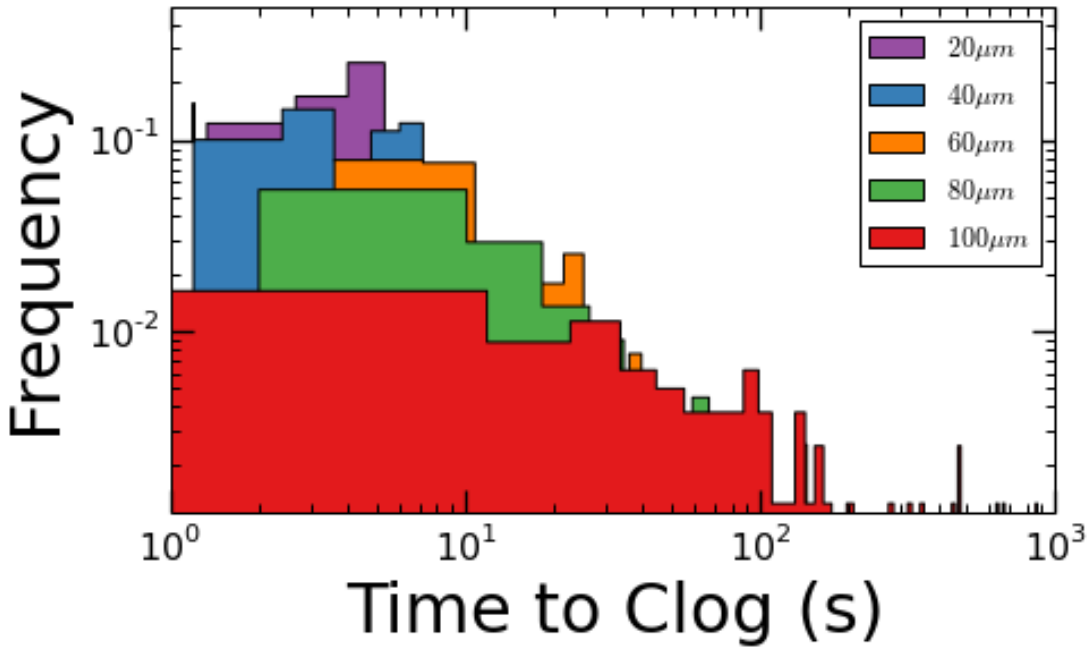

Figure 2.8: Normalized histograms of clogging times for microchannels with mouth widths varying from $20\mu m$ to $100\mu m$.

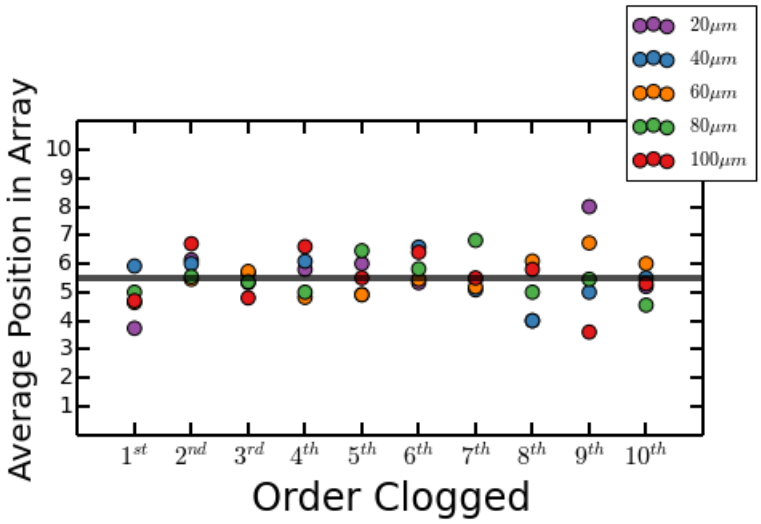

Figure 2.9: A graph of Average Position in Array vs. Order Clogged. Graph shows that clogging is not strongly influenced towards the left or right side.

and ten, where one is the leftmost channel in the array and 10 is the rightmost channel in the array. We then compute the average value of the first channel to clog in each array. If the likelihood for each channel to clog is roughly equal, we expect the average value of the first pore clogged to be close to 5.5 which is equal to the average of the set of numbers one through ten, inclusively. We also compute the average value for the second channel to clog, the third channel to clog and so on until the 10th channel is clogged. We find that the average value, or average position, oscillates closely around 5.5 for each ordinal clogging position as shown in Figure 2.9. Therefore, the tendency of a channel to clog is not dependent upon its spatial position in the array.

We complete a similar analysis to analyze whether the distance from the wall influences channel clogging. We assign the channels to groups determined by their distance from the wall. Channels that are closest to the wall and previously label #1 and #10 are now considered group #1. Channels previously labeled #2 and # 9 are now group #2 and so forth. We compute the average group number for each ordinal position clogged (first through tenth) as shown in Figure 2.10. If each group has

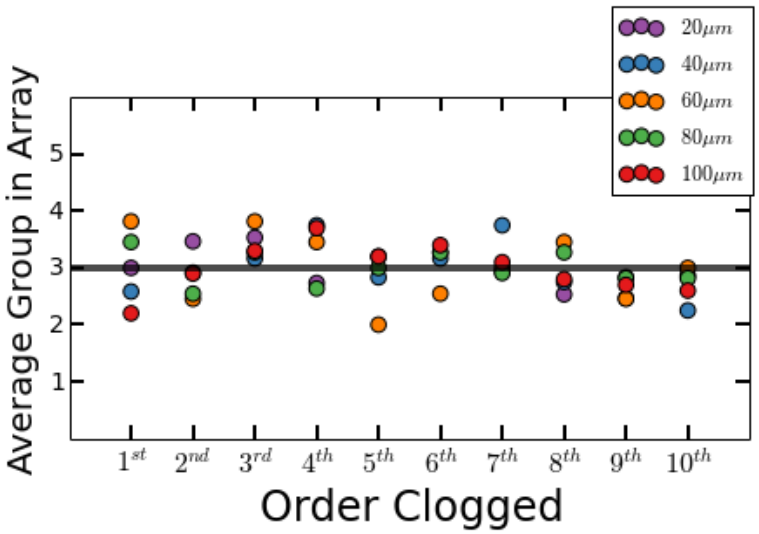

Figure 2.10: A graph showing the Average Group Value vs. the Order clogged. Group one is comprised of the leftmost and rightmost channels while group 5 is composed of two innermost channels. This graph shows that proximity to wall does not strongly influence clogging.

an equal chance of clogging first, we expect the 1st channel in the array that clogs to have an average group number of 3 (the average of the numbers one through 5. In our experiments the average group value of ordinal position oscillates closely around 3 as shown in figure 2.10.

Based on these observations, we conclude that a channel's spatial location in the array does not strongly influence its tendency to clog. Assured of the independence between a channel's clogging behavior and array position; we now calculate the number of particles that pass through the channel prior to clogging.

Using our measurements of time elapsed before clogging, we calculate the number of particles that pass before clogging using two methods. The two methods produce approximations that agree within 50%. However, the first method, which utilizes a calibrated length of tubing produces estimates that are consistently higher than the method that relies upon the channel resistance. The difference in the estimates likely results from an over estimation of the of the flow rate through the

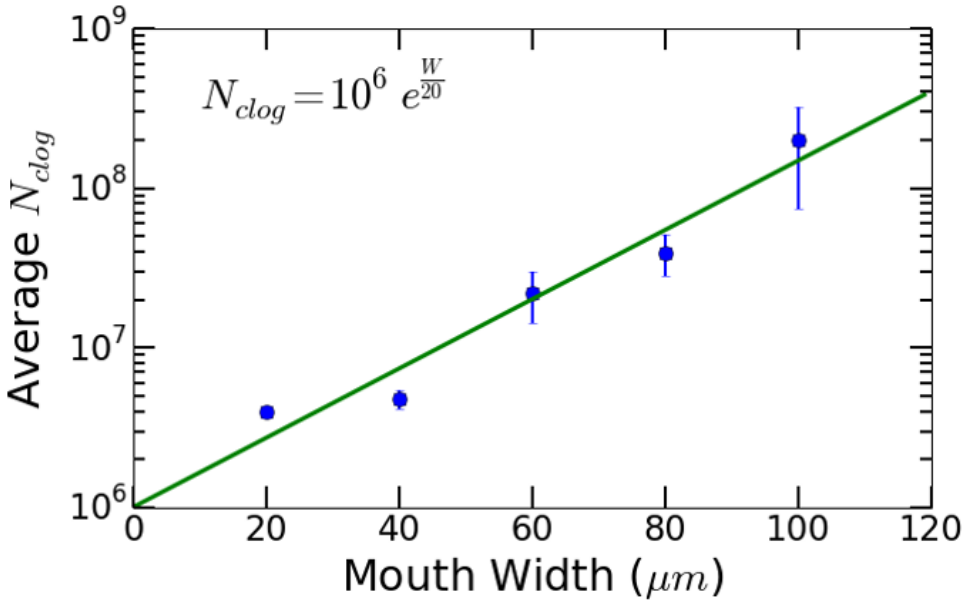

Figure 2.11: A plot of average number of 3 μm diameter particles, N*, that pass through a1200 μm long channel before clogging vs. the channel mouth width. An exponential curve fits the data well. This graph shows that that mouth width strongly affects clogging behavior of a tapered channel.

calibration tubing when only one channel in the array is unclogged.

The average of the two methods, N*, provides a good estimate of the total number of particles that pass through a channel before it clogs. N* increases exponentially as the mouth width increases linearly. Applying an exponential fit yields a characteristic length of 20 μm according to Equation 2.3. This value of 20 μm is very close the characteristic length of the channel's constriction $l_c = (2w + 2h)/4$.

$$N_{clog} = 10^6 e^{\frac{W}{20}} \tag{2.3}$$

Although our data fit an exponential model quite well for 3 μm diameter particles previous clogging models do not account for the exponential relationship. To gain further clarity we also test the clog-

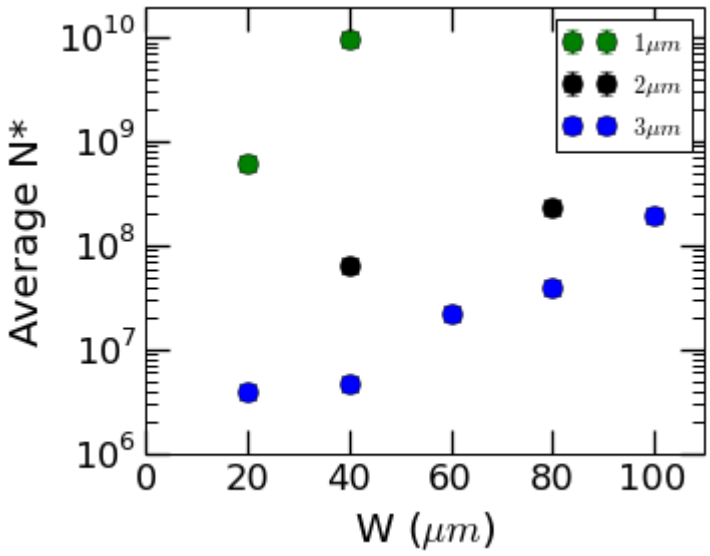

Figure 2.12: A graph showing the Average Number of 1 μm, 2 μm and 3 μm diameter particles, N*, that pass through a channel before clogging vs. the channel mouth width. All channels are 1200 μm long. This graph demonstrates that smaller particles are less likely to clog which comports with results from literature [30,20].

ging behavior of 1 μm and 2 μm diameter particle suspension that have identical volume fraction and driven using the same pressure. As expected, the suspensions containing 2 μm diameter particles pass more particles prior to clogging than 3 um particulate solutions while suspensions of 1 μm diameter particles require the most particles to flow through a given channel prior to clogging. We attempt to scale our results using the scaling law previous reported [30]. We find that tapered channels do not scale in a similar manner as channels used in the reported studies.

We continue testing the effect of channel geometry on clogging behavior by varying the length of a microchannel with a fixed taper rate. We choose a taper rate that decreases the channel width by 1 µm per 30 μm channel length, which is the same taper rate as the channels whose width decreases from 40 μm to 10 μm over 1200 μm. Maintaining a constant rate of taper and a constant height of 25 μm, we fabricate three sets of channels: Channels that are 900 μm long and have 33 μm wide entrance, channels that are 600 μm long and have a 25 μm wide entrance and channels that are

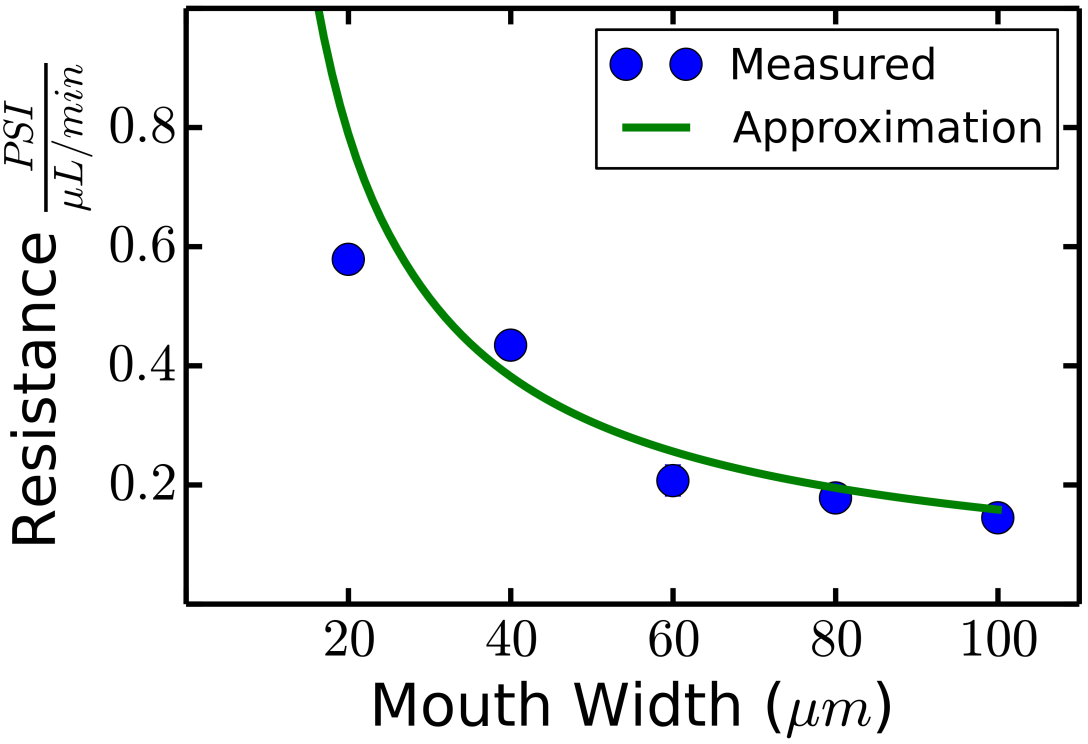

Figure 2.13: Plot showing hydro- dynamic resistance vs. Mouth width for 1200 μm long tapered channels with varying mouth width.

300 μm long and have a 18 μm wide entrance. The average number of particles that pass through a channel prior to clogging decreases linearly as the length of the channel decreases with a slope of $4.9 \times 10^4 \mu m^{-1}$ as shown in Figure 2.15.

Channel length was not considered by previous experimental studies and we are unable to directly compare these results to an established model. Instead we connect the hydrodynamic properties of our channels to the observed clogging behavior.

In tapered channels with a constant length, N* increases exponentially as the mouth width increases linearly (Figure 2.11) whereas the hydrodynamic resistance of channels is inversely proportional to the mouth width ((Figure 2.13). To make a parallel comparison we measure the resistance of the

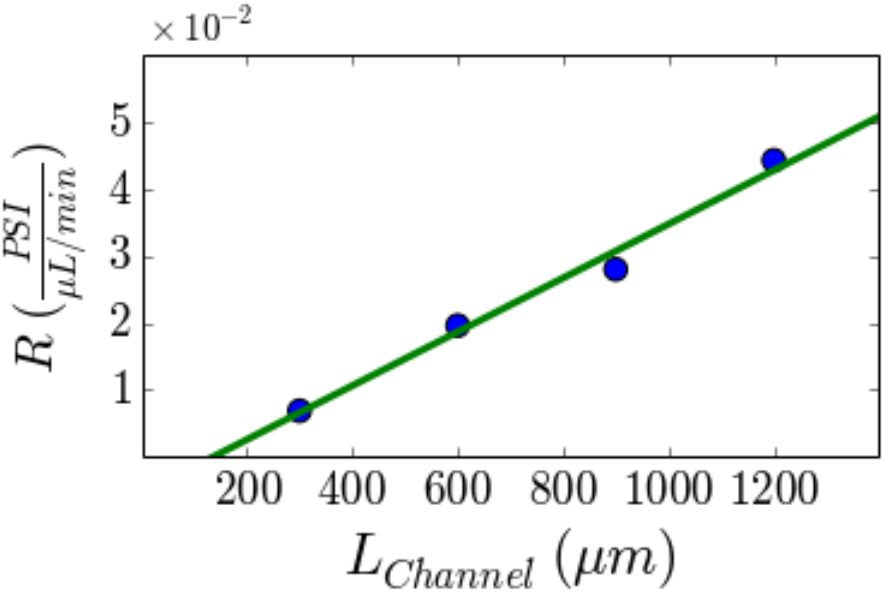

Figure 2.14: Graph of the Average Number of 3 μm diameter particles, N*, that pass through a channel before clogging vs. the Channel Length. Each channel has the same taper angle as a channel whose width decreases from 40 μm to 10 μm over 1200 μm. Graph shows that longer channels are more likely to clog.

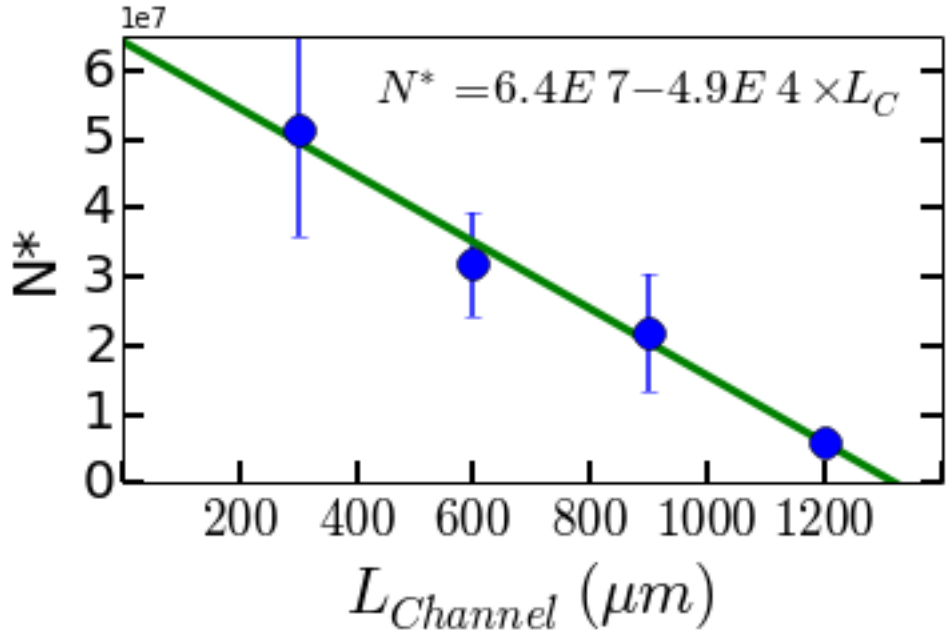

Figure 2.15: A graph showing Channel Resistance vs. Channel Length for channels that have the same taper angle as a channel whose width decreases from 40 μm to 10 μm over 1200 μm. Channel resistance increases as channel length increases.

channels that have a decreasing channel length but a constant taper rate. Interestingly, the measured hydrodynamic resistance increases linearly with increasing channel length whereas N* decreases linearly with increasing channel length. Because our experiments operate at the same applied pressure, the flow rate through each microchannel is proportional to is resistance. Therefore, our results point to a relationship between N* and the flow rate of the passing suspension.

We investigate the role of flow rate in clogging by altering the pressure applied to channels whose width tapers from 40 μm to 10 μm over a length of 1200 μm. In these experiments we use 30 channel arrays to maximize the number of data points per experiment. We increase the pressure from 3.4 kPa to 28 kPa and estimate the number of particles that pass before clogging[‡]. N* increases with

[‡]In these experiments we only utilize the method involving channel resistance to estimate N*

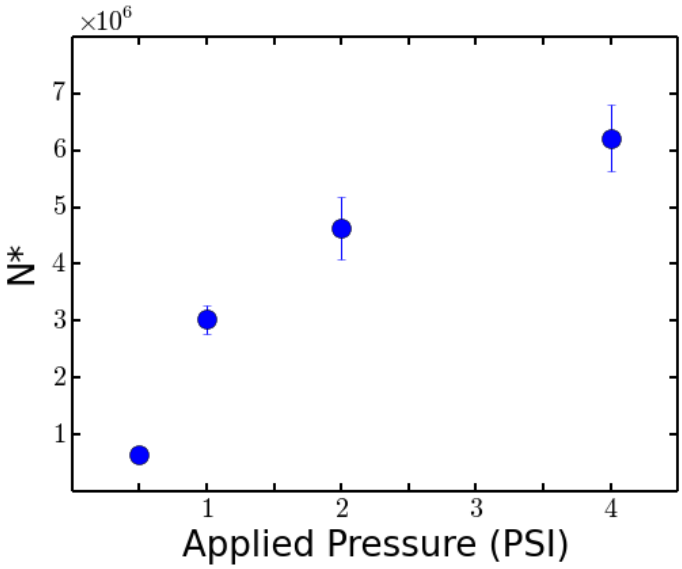

Figure 2.16: A graph showing Average N* vs. applied pressure, p_a for an array of 30 micochannels whose widths decrease from 40 μm to 10 μm over 1200 μm. Clogging decreases with increasing pressure until 2 PSI. Between 2 PSI and 4 PSI there is little change in clogging.

increasing applied pressure.

Pressure applied to the suspension is directly proportional to the suspension's flow rate through the channel and hence our results confirm the idea that increasing the flow rate through a channel decreases that channel's likelihood of clogging. As the suspension's flow rate through the channel increases, the average velocity of the suspension through the channel increases as well. Although the average velocity through the channel increases with pressure, the fluid velocity at the channel walls remains zero, due to the no-slip condition. Hence, the gradient of the velocity increases as the applied pressure increases. The near wall velocity gradient is directly proportional to the near wall shear stress, as shown in equation 2.4.

$$\tau = mu\frac{dU}{dx_\perp} \tag{2.4}$$

The near wall shear stress engenders a force on particles near channel wall, pushing the particles away from the way. Thus the near wall shear stress limits particle adhesion to the wall. Particles that are less likely to adhere to the wall are less likely to aggregate on the wall and engender clogging. As a result, particles that experience higher shear stresses in the channel, are less likely to form clogs. Therefore, increasing the flow rate of a suspension through a channel allows more particles to pass before that channel clogs.

Being a scientist requires having faith in uncertainty, finding pleasure in mystery and learning to cultivate doubt. There is no surer way to screw up an experiment than to be certain of its outcome.

Stuart Firestein

3

Clogging in Single Tapered Microchannels

We saw unexpected clogging behavior in arrays of 10 microhannels in the preceding chapter. Unlike previously published experiments that utilized uniformly varying microchannels, tapered microchannels are less likely to clog in response to increasing flow rate. We connect the change in clogging behavior resulting from increased flow rate to increasing shear stress that hinders particle adhesion which induces clogging. However, due to the resolution limit inherent to imaging 10 channels at once, we could not resolve individual particles behavior in the channels. When individual particles are not resolved, the clogging mechanism cannot be resolved and hence the mechanism cannot be visually confirmed. These limitations stymied our ability to deeply understand the clogging behavior witnessed in the previous channel. Previously published studies on clogging in microchannels used even larger arrays of channels and also did not resolved single par-

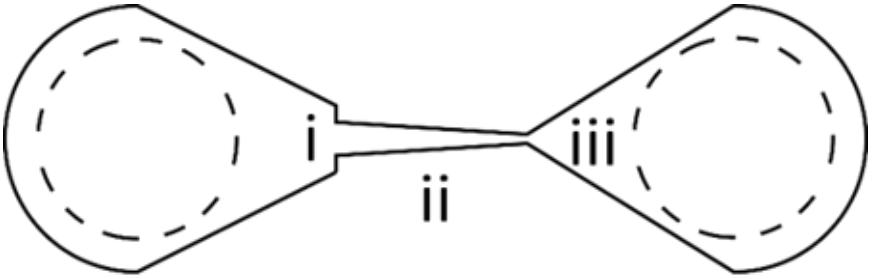

Figure 3.1: Illustration of the microfluidic device with channel used for clogging The mouth width, (i), is 40 μm wide, the channel is $\mu 300 \mu m$ and the constriction is 10 mum wide.

ticles nor image the clogging mechanism.[30,20,2,23] In this chapter, we present the first experimental study of microscale clogging in which single particles are resolved using single microchannels. In the single microchannels, we examine how clogging behavior changes in response to changes in the flow rate through the channel and changes in the particle interactions.

3.1 Experimental Methods

Single microchannels are again fabricated using printed photolithography masks for later use in the soft lithography fabrication process. In CAD software we draw 2-Dimensional patterns that begin with round 1.5 mm inlet areas that decrease linearly to a width of 60 μm. At this point, the channel width steps from 60 μm to 40 μm and the tapered channel begins. The initial width of the tapered channel is 40 μm and decreases linearly to a 10 μm throat width over a length of 300 μm. After the 10 μm constriction, the channel pattern gradually opens back up to a 1.5 mm round outlet area. The CAD drawings are printed on Mylar in the negative at a 10 μm resolution.

Once printed, the masks are used to create channel molds in SU-8 3010 photoresist. The photoresist is spun onto cleaned silicon wafers at a 1000 rpm to leave a 15 μm thick layer. The wafer then pre-bakes on a hot plate (VWR) for 10 minutes at 95^{0}C and after cooling 200 $\frac{mJ}{cm^2}$ of ultraviolet light is shown through the photomask onto the photoresist. Next, the wafer is post-baked on a hot plate for 1 minute at 65^{0}C, 4 minutes at 95^{0}C and then developed in PGMEA for six minutes. After rinsing

the photoresist with PGMEA and then with Isopropanol Alcohol (IPA), it is placed into a plastic petri-dish. Liquid PDMS elastomer is mixed with crosslinker at a 10:1 ratio and poured onto the wafer. After baking in an oven (VWR) for at least 1 hour at 65^{o}C, a PDMS section containing the imprinted channels is cut and peeled from the wafer. Next, 1.20 mm holes are punched into the PDMS using a biopsy punch and the PDMS chip then undergoes a cleaning process. Initially, the transparent tape (Scotch-3M, St. Paul Minnesota) is used to lift PDMS fragments and dust from the PDMS chips and glass slides. Next, the PDMS chips are then submerged in an IPA bath that is sonicated for 2 minutes (Branson) before finally being dried with nitrogen and baking in a 65^{o}C oven for at least two minutes. Separately, glass slides are cleaned using acetone (Sigma Aldrich), lint free wipes (VWR) and IPA.

The glass slide and PDMS chip are placed in a Plasma System (Diener, Ebhausen, DE) and exposed to an oxygen plasma for 10 s. Immediately after removing the two pieces from the plasma chamber, the PDMS chip and glass slide are pressed together. After a few minutes, the two pieces are bonded together. Exposure to oxygen plasma temporarily changes the surface energy of materials. However, the change in surface energy due to oxygen plasma decays to an imperceptible level[25] 15 hours after exposure. Therefore, the newly formed microfluidic chips rest for at least 24 hrs before the surface is further modified.

The microfluidic devices are treated with 0.1 M sodium hydroxide for 1 minute before rinsing with distilled water and flushing with nitrogen. Then a 1 % (wt/wt) poly diallydimethylammonium (polyDADMAC) in 2M sodium chloride solution is applied for five minutes. After rinsing with distilled water and blowing with nitrogen, the surfaces of the microfluidic devices are coated with the cationic polyDADMAC which effectively renders the surface positively charged. A negatively charged surface is created by applying a solution of 1% poly sodium styrene sulfonate (PSS) in 2 M NaCl for 5 min. to a surface that has a layer of adsorbed polyDADMAC. The negative surface is created when a layer of PSS adsorbs onto the polyDADMAC.

We use pressure to drive particulate suspension through the microchannel. The particulate suspension reservoir is enclosed in an airtight Pyrex bottle whose cap permits the entrance of air via a Luer hole and the withdrawal of liquid by a hole for a $1/16^{th}$ outer diameter polymer tubing. One end of the $1/16^{th}$ outer diameter (0.030 inch inner diameter) tubing connects to the inlet while the other end rests submerged in the particulate suspension. The height of the suspension is always matched to the height of the microfluidic chip to prevent gravity induced flow. We pressurize the bottle at levels ranging from 690 Pa (0.1 PSI) to 6.9 kPa (1.0 PSI) which forces the suspension through the tubing, through the microchannel and eventually out to a waste beaker that is held at atmospheric pressure. We observe the suspension flowing through the microchannels using optical microscopy (Nikon) and record the behavior at 10 fps (Fastec). Before the particulate suspension flows through a channel, the channel is flooded with a liquid identical to the continuous phase of the suspension. The initial channel flooding prevents pockets of air that form in the channel if the particle suspension enters a dry channel.

The particulate suspension is comprised of 2.1 μm diameter polymerized methacrylate (Figure 3.3) suspended in water. The particles are made of a copolymer of triuoroethyl methacrylate and tert-butyl methacrylate and stabilized with the anionic monomer 3-sulfopropyl methacrylate which has a length on the order of a nanometer. A portion of these particles also have the 50 nm long neutral polymer, N,N-dimethylacrylamide polymers grafted from the particle surface to provide steric stabilization. In addition to pure water, a portion of the particles are suspended in potassium chloride solutions ranging from 100 μM to 2.5 M.

3.2 Results and Discussion

Before we begin clogging the microchannel, we measure the hydrodynamic resistance of the microchannel. Using a syringe pump (Harvard Apparatus, MA), we flow water at a controlled flow rate through the microfluidic device. We vary the flow rate from 5 μL/Hr to 600 μL/Hr.

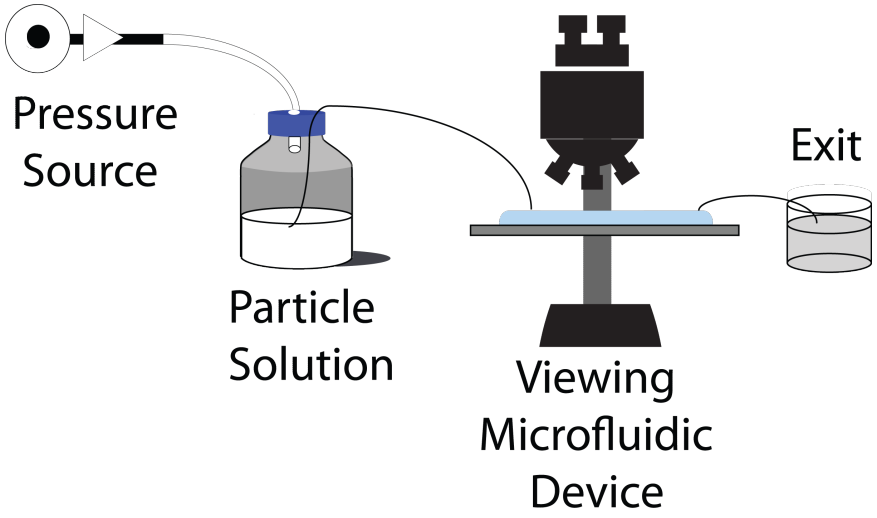

Figure 3.2: Schematic of experimental apparatus. Compressed air pressurizes a glass bottle containing particulate suspension. After the bottle pressurizes, the suspension flows into the submerged tubing out of the bottle the microchannel which is watched by a microscope and eventually flow out into a waste beaker.

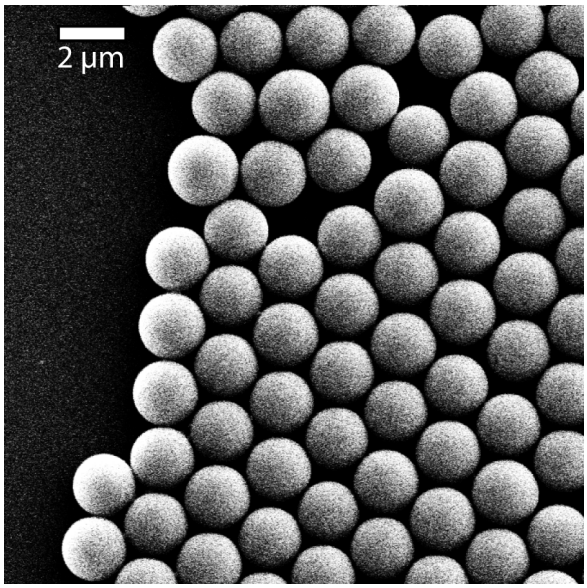

Figure 3.3: Scanning Electron Microscopy image of electrostatically stabilized particles made of PMMA. Particles are 2.1 μm in diameter.

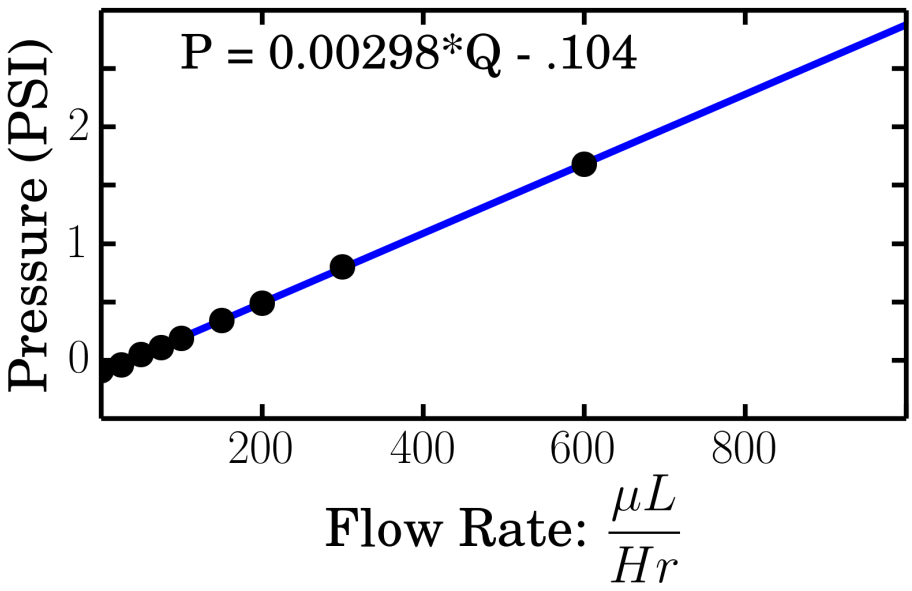

Figure 3.4: A plot of Pressure difference vs. Flow Rate across a microfluidic device containing a single microchannel that is 300 μm long, 15 μm deep and has a width that decreases from 40 μm to 10 μm. A linear fit gives the slope.

We connect pressure transducers to the inlet and outlet of the microchannel with 1/16th outer diameter (0.030 inch inner diameter) tubing to measure the pressure difference across the microfluidic device while water flows through the channel. As we increase the flow rate using the syringe pump, the pressure difference across the channel increases. When plotted, the slope of this line reveals a hydrodynamic resistance $2.98 \times 10^{-3} \frac{PSI}{(uL/min}$. We use this hydrodynamic resistance to estimate the initial flow rate through our microchannels when we use pressure to drive particulate suspensions through a channel. In our experiments the initial flow rate varies between 34 μL/Hr and 670 μL/Hr.
When we flow anionic particles through a channel with an anionic polyelectrolyte layer, the particles do not stick to the channel walls. The like charge between the particles' surface and the channel walls causes a Coulombic repulsion between the two and prevents adhesion. Without adhesion, particles are unable to build up on the channel walls and obstruct flow. Consequently, the particulate solu-

tion flows unobstructed for more than one hour, at which point we manually stop the stream. By contrast, anionic particles will adhere to the channel walls if the walls have only been coated with a layer of cationic polyelectrolytes. As more particles channel stick to the walls, the channel becomes obstructed by a packing of particles and clogging ensues.

We define a clogged channel to be one which no longer permits particles to exit the channel constriction due to a packing particles in the channel. Although the channel is clogged, fluid still traverses through the clogged microchannel. Fluid continues moving through the spaces between the particles that pack together in the channel. The size of voids in the particle packs is smaller than the particle's diameter and only a small volume of fluid can flow through a clogged channel. Therefore, the flow rate through a clogged channel is small compared to the flow rate through the channel just before clogging and the fluid velocity of through a clogged channel very small. This decrease in fluid velocity is evident in the last particles that exit the channel before it clogged. These particles continue to move away from the constriction after the channel clogs, but at a much lower velocity.

Using our definition of clogging, we measure the total time the suspension flows through each channel before clogging ceases. At applied pressures below 3 kPa, the average time to clog a channel increases as we increase the pressure applied to the particle suspension as shown in Figure (3.4). At pressures higher than 3 kPa, the average time to clog dramatically decreases.

In contrast to our observations, traditional clogging models[30] predict that clogging time will decrease in response to increasing applied pressure, not increase. Thus traditional clogging paradigms cannot be used to explain our results. The sudden decrease in clogging times at pressures greater than 3 kPa is also surprising due to its contrast from clogging times at lower pressures. When examining the increasing clogging time below 3 kPa and decreasing clogging time above 3 kPa, we notice that the change in the uncertainty in the clogging time mirrors the change in clogging time as shown in Figure 3.4. As the applied pressure grows to 3 kPa, the uncertainty increases. Whereas when pressure grows larger than 3 kPa, the uncertainty also decreases. The surprising trends in the average

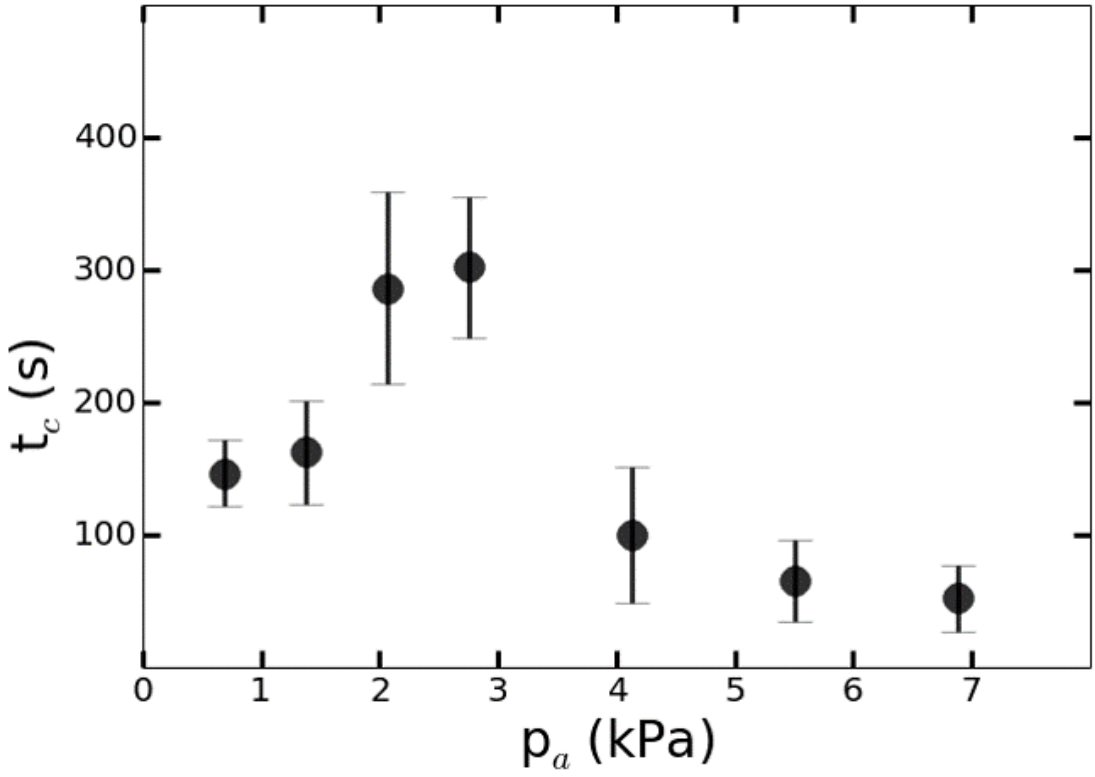

Figure 3.5: A plot of time to clog vs. applied pressure. At low applied pressures, the average time to clog increases as the applied pressure increases. At higher pressures, the time to clog decreases with increasing pressure.

clogging time and the corresponding trends in the uncertainty of the average clogging time suggests that the clogging behavior is not well described by an overall average of the clogging time. Our results therefore warrant a closer inspection of each clogging experiment.

Using the movies of individual microchannels clogging at 10 fps, we spatially and temporally resolve the clogging behavior of each microchannel. Upon close inspection of each video we observe the presence of two distinct types of clogging events. In the first type, we see particles successively adhere near the constriction. This buildup obstructs the channel near the constriction and causes clogging, as schematically shown in Figure 3.6. The successive particle adhesion appears in the formation of a black layer along the channel walls in the optical micrograph in Figure 3.6. In the second type, we see particles adhering upstream from the constriction. The particles aggregate on the wall, detach and flow into the constriction causing a clog as shown schematically in Figure 3.6 and on the optical microscope image in Figure 3.6.

We categorize each clogging experiment by monitoring the experiment for the presence of particle clusters. If there are moving clusters in the flow, the clog is classified as forming due to particle clusters. If we observe no clusters moving in the channel, we classify the channel as having clogged via the buildup of single particles. For each applied pressure, we calculate the average time required to clog a channel for each mechanism. When clogging is caused by the first mechanism, a buildup of particles near the constriction, the average time to clog increases as applied pressure increases as shown in Figure 3.7. By contrast, the average time to clog decreases with increasing applied pressure if particle clusters engender clogging, as is the case for the second mechanism.

Like other clogging events, these inverse behaviors result from the competing forces of hydrodynamic drag and adhesion. At higher applied pressures, the flow rate through the channel is higher resulting in a higher maximum velocity in the channel. Although the maximum velocity increases with pressure, the velocity near the wall remains near zero due to the no-slip condition. Therefore, the velocity gradient perpendicular to the wall increases at the pressure increases and a larger velocity

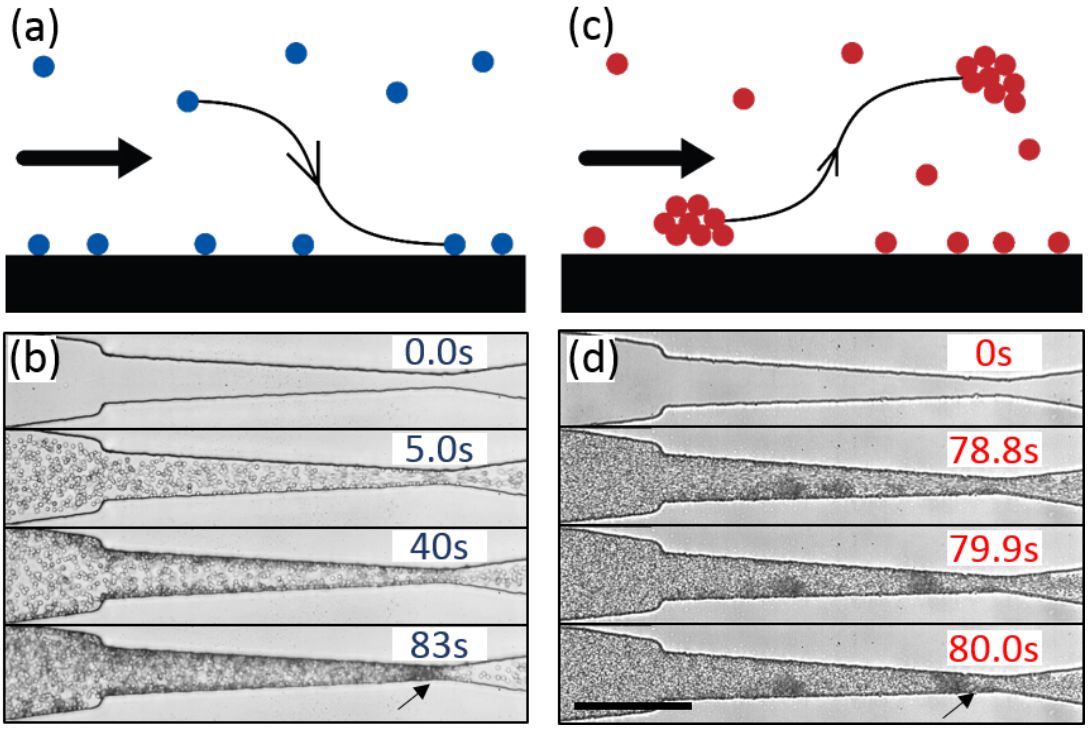

Figure 3.6: (a) Sketch of clogging due to the buildup of single particles. (b) Micrographs of clogging caused by single particles accumulating near the constriction. (c) Sketch of particle cluster detachment. (d) Micrographs of clogging caused by a detaching particle cluster. Scale bar represents 100 μm. Arrows indicate location of clog.

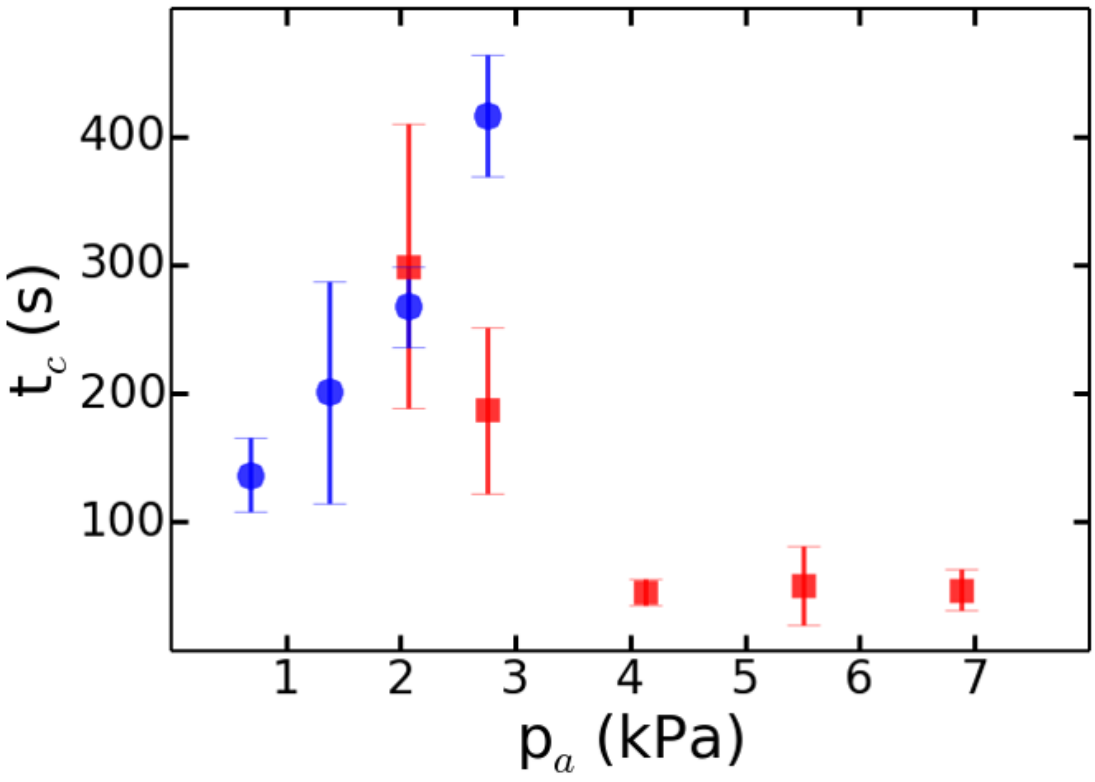

Figure 3.7: Plot of time to clog vs. applied pressure. Clogging by the accumulation of single particles near the constriction is represented by blue circles and clogging by clusters of particles is represented by red squares.

gradient imparts a larger shear stress on particles in the channel as shown in equation 2.2. The higher shear stress causes the particle clusters to detach from upstream walls before individual particles attach to the walls near the constriction. The competition between particle cluster detachment and single particle adhesion highlights the particle-wall interaction as an important parameter for further exploration.

To probe the role of the particle-wall interactions we use particles with differing surface stabilization. We use particles that have only electrostatic stabilization and we also use electrostatically stabilized particles that have a neutral molecule adsorbed onto the surface rendering it electrosterically stabilized. These particles are the same size as used in previous experiments and are suspended in water or solutions of potassium chloride (KCl) in water at a fraction of 12 % (w/w). We vary the molarity of the KCl-H_2O solutions from 100 μM to 2.5 M. We then then flow the particle suspension through channels with the same geometry as used in previous experiments using an applied pressure of 1.4 kPa.

In the absence of salt, both particle types clog in an average time 10 s as shown in Figure 3.8. If dispersed in solutions containing more than 100 μ M of salt, the electrosterically stabilized particles do not clog the channels within the 1000 s observation time. When dispersed in solutions containing of 50 mM of salt, the electrostatically stabilized particles require hundreds or thousands of seconds to clog or sometimes do not clog the channel within the 1000 s observation time. At salt concentrations greater than 50 mM, the electrostatically stabilized particles do not clog within the 1000 s observation time.

The surfaces of both particle types contain charge groups leading to an attractive electrostatic interaction between the anionic particles and channel walls which are covered with cationic particles. The addition of salt creates dispersed ions that screen electrostatic interaction. This electrostatic interaction decays exponentially a with characteristic length, the Debye length,[7] according to:

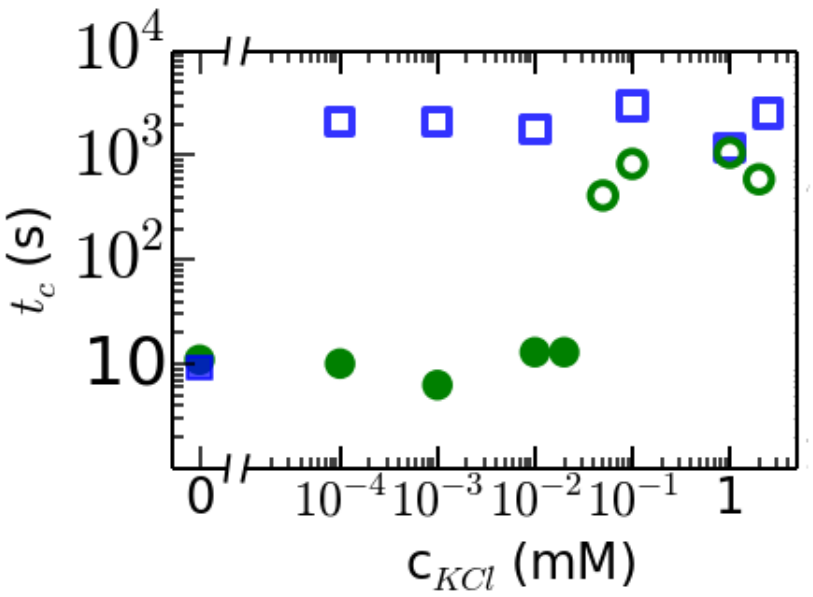

Figure 3.8: A plot of the Average Clogging Time vs. Concentration of Potassium Chloride in Water (c_{KCl}) at an 1.38 kPa applied pressure for electrostatically stabilized particles (green) and electrosterically stabilized particles (blue). Open circles indicate that clogging was not observed. The electrostatically stabilized particles ceasing clogging at 50 mM while the electrosterically stabilized particles cease clogging with the addition of a small amount of salt.

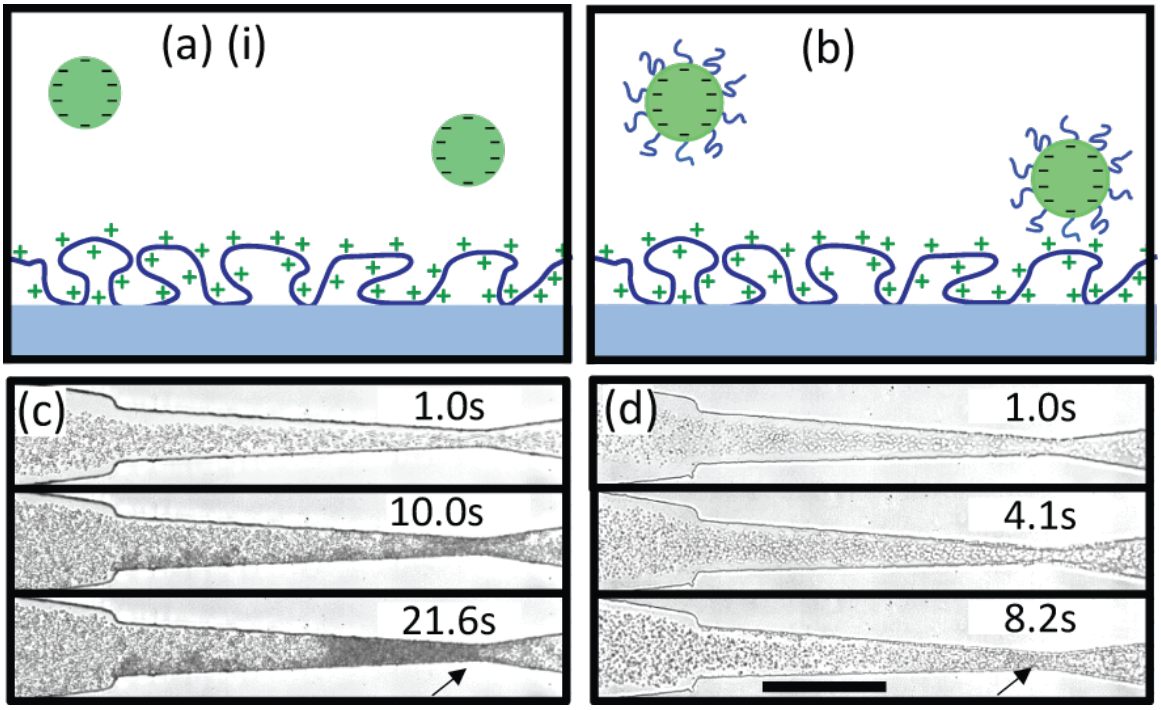

Figure 3.9: Sketch showing negatively charged (a) electrostatically stabilized particles and (b) electrosterically stabilized suspended in water near a positively charged poly-electrolyte layer adsorbed onto a surface in the presence. The micrographs in (c) show clogging of electrostatic particles suspended in water. The micrographs in (d) show clogging of electrostatic particles suspended in water. Arrows indicate the location of clogs. The scale bar represents 100 μm.

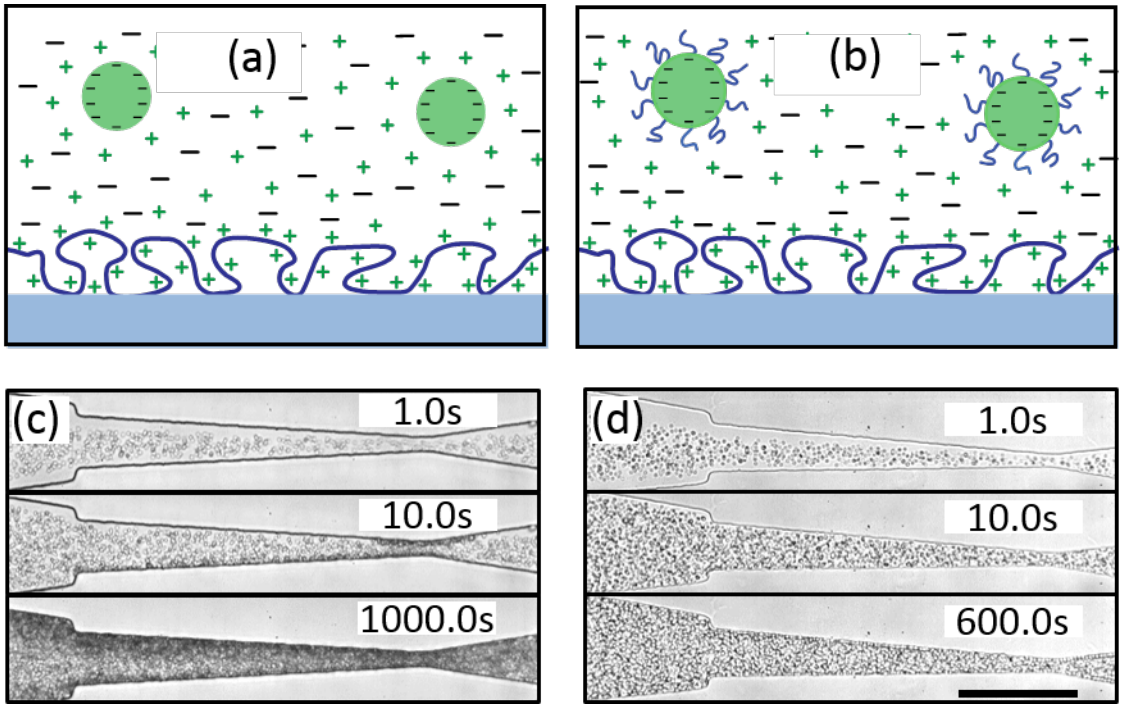

Figure 3.10: Sketch showing negatively charged (a) electrostatically stabilized particles and (b) electrosterically stabilized suspended in an electrolyte solution near a positively charged poly-electrolyte layer adsorbed onto a surface in the presence. The micrographs in (c) show clogging of electrostatic particles suspended in a mM KCl in water solution. The micrographs in (d) show clogging of electrostatic particles suspended in a 500 mM KCl in water solution. Clogging was not observed in (c) and (d). The scale bar represents 100 μm.

$$\kappa^{-1} = \sqrt{\frac{\varepsilon_r \varepsilon_0 k_b T}{2 N_A e^2 I}} \tag{3.1}$$

The electrosterically stabilized particles no longer clog when the added salt concentration creates a Debye length approximately equal to the length of the steric polymer adhere to the surface of the particle as shown in Fig. 4. Surprisingly, the electrostatically stabilized particles also cease clogging when the Debye length is approximately the size of the much smaller, charged molecule that is adsorbed onto the surface of the particle. Thus clogging can be completely stopped by modulating the electrostatic length of interaction which affects ability of particles to stick to channel walls.

Our results again affirm the prominence of particle adhesion in the process of clogging. In this chap-

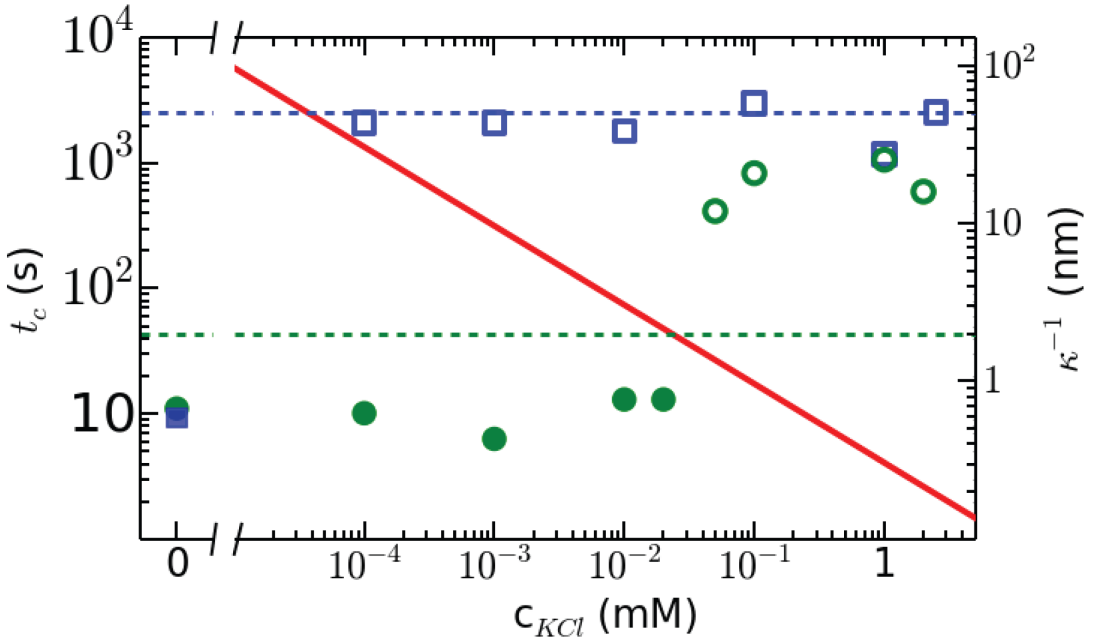

Figure 3.11: A plot of the Average Clogging Time and Debye Length vs. Concentration of Potassium Chloride in Water (c_{KCl}) at an 1.38 kPa applied pressure for electrostatically stabilized particles (green) and electrosterically stabilized particles (blue). The red line represents the Debye Length. Open circles indicate that clogging was not observed. The electrostatically stabilized particles ceasing clogging at 50 mM while the electrosterically stabilized particles cease clogging with the addition of a small amount of salt. The red line represents the calculated Debye length for a monovalent salt in water. The blue dashed line indicates the length of steric polymer while the green dashed line indicates the length of the electrostatic molecule. The electrosterically stabilized particles cease clogging when the Debye length is less than 50 nm while the electrostatically stabilized particles cease clogging when the Debye Length is on the order of 1 nm.

ter we used hydrodynamic induced shear force to probe the tendency of particles to adhere to channel walls in the constriction or detach in clusters from upstream channel walls. We then modified the effective length of the electrostatic interaction to prevent particles from attaching to the channel walls. Whereas changing the flow rate through the channel engenders switching between clogging mechanisms, we show that salt concentration can switch off clogging by decreasing interaction distance between particles and surfaces.

Ignorance follows knowledge, not the other way around.

Stuart Firestein

4

Conclusions and Outlook

This dissertation explores clogging at the microscale using microfluidic channels and colloidal particles as a model system. In Chapter 1, we discuss the general process of clogging and the prevalence of clogging in a range of industrial processes. We present the idea of a micromodel to overcome the limitations encountered when studying clogging in situ. Our model can reflect multiple clogging scenarios when the micromodel's parameters are varied. In each of the experiments presented in this dissertation, we analyze the clogging behavior of tapered microchannels instead of the uniformly varying microchannels of earlier studies. Over the course of this dissertation, we alter a variety of parameters that are either thought to have little effect on clogging or are unperturbed by preceding studies.

4.1 Conclusions

In Chapter 2, we focus on the effects of varying channel geometry. While maintaining a constant height and constriction width, we vary: the particle size, taper angle, channel length and pressure applied to the suspension. We test three particles sizes and find that smaller particles are less likely to clog channels which is in agreement with results from literature[30]. We proceed to test the clogging behavior channels with different mouth widths, but constant channel height, particle size and applied pressure. The number of particles that pass before clogging increases exponentially with increasing mouth width. We see a strong positive correlation between the dimensions of the channel upstream constriction and the average number of particles that pass through a channel prior to clogging even when the constriction is the same size among all channels. However, when we vary the mouth width of the tapered channels while holding other parameters constant, we simultaneously vary the volume of the channel and the taper rate of the channel.

To isolate the effect of the upstream channel volume on clogging behavior, we clog channels with the same taper rate and variable channel length. When the channel's taper rate is constant but the upstream channel volume increases, the channels clog more readily. The number of particles that pass through channels with a constant taper rate increases linearly with increasing channel length. In contrast to the variable mouth width channels, increasing the upstream volume while maintaining a consistent constriction increases the likelihood of clogging.

These seemingly contradictory results point to another culprit that influences clogging in tapered channels: hydrodynamic resistance. For channels of identical length and constriction width, increasing the mouth width decreases the channel's hydrodynamic resistance. Decreasing the length of channels with an identical taper rate also decreases the channel's hydrodynamic resistance. As the channel's hydrodynamic resistance increases, the number of particles that pass before clogging decreases. The flow rate through a channel is directly proportional to the pressure applied across the

channel and the channel's hydrodynamic resistance. Hence our channels are less likely to clog when the suspension is flown at higher rates.

We then confirm our observation by testing the influence of flow rate on clogging by varying the pressure applied to the particulate suspension. At the lowest flow rates, an increase in flow rate corresponds to an increase in the number of particles that pass through a channel before clogging. These results affirm our previous results and illuminate the importance of a variable that was given little thought in previously published work. We explain the importance of flow rate via its connection with shear force. At higher flow rates, the particles experience higher shear forces, especially, in the constriction. The higher shear forces deter particles from approaching and adhering to channel walls, a prerequisite for clogging.

To conclude Chapter 2, we consider the clogging behavior when the suspension's flow rate increases to the highest levels we are able to test. Unlike at low flow rates, the number of particles needed to pass before clogging at the highest flow rates shows very little increase. We are unable to fully explain this behavior because our experiments are not imaged at sufficiently high resolution due to the numerous channels used. Also, we do not test other parameters that influence sticking behavior.

In Chapter 3 we image the clogging behavior of individual, tapered microchannels at a resolution high enough to image individual particles. In these experiments we do not alter the channel size or geometry. Once again, we apply a constant pressure to drive the flow through our microchannels and we vary the applied pressure to alter the flow rate. Instead of using commercially available microparticles, we fabricate particles and with two different types of surface functionalization for comparison. We also adjust another parameter, the surface potential, by adsorbing polyelectrolytes onto the channel walls. When we flow negatively charged particles through a channel whose walls are coated with anionic polyelectrolytes, the channel does not clog. Conversely, when we flow the negative particles through channels with cationic particles, clogging ensues.

We observe that at low applied pressures the time to clog a single channel increases as the applied

pressure increases. At higher pressures, however, the time to clog decreases as the applied pressure increases. Closely examining each clogging event reveals two distinct clogging mechanisms that respond differently to changes in flow rate. At low pressures we find that clogging occurs via the buildup of single particles but at high pressures, clogging results from detaching particle clusters. Each clogging mechanism corresponds to a trend in clogging time. Clogging via the buildup of single particles requires more time as the applied pressure increases, whereas, clogging via cluster detachment proceeds more quickly as the applied pressure increases.

These inverse behaviors most likely result from the competing shear force and adhesion force. At low applied pressures, the particles move slowly throughout the channel allowing particles to adhere and build up near the orifice. Increasing applied pressure to the particle suspension speeds up the particles and hinders their sticking ability, especially near the constriction where particles move most quickly. Thus at higher applied pressures, particles require more time to accumulate on the channel surface, increasing the average clogging time. At even higher pressures, particles are unlikely to adhere to channel walls near the constriction but they still adhere to upstream channel walls where the channel is wider and thus the particles travel more slowly. As more particles adhere and form a particle cluster on the channel wall, the fluid flowing around the cluster exerts a drag force on the cluster and eventually detaches it. Once detached, the cluster can flow into the constriction and engender a clog. Particles detach more readily as the drag force increases due to increasing applied pressure. Thus as applied pressure increases, particle clusters detach more readily and clogging time decreases.

Also in Chapter 3, we test the role of particle-wall interactions by clogging particles with different surface stabilizations in the presence of salt. Particles with short, negatively charged molecules on the particle surface clog in the absence of salt and at low salt concentrations. When salt is added at a concentration of about 50 mM, clogging ceases. Particles with short, negatively charged molecules and long neutral molecules attached to the surface clog in the absence of salt. However, clogging with these particles ceases with even small additions of salt. We attribute the difference in clogging

behavior between the particle types to the length of the stabilizing molecules on the particle surface. The particles are able to adhere to the polyelectrolyte coated surface until the length of interaction between the particle surface and channel surface is comparable to the length of stabilizing molecule. When the two lengths are comparable, particles no longer adhere to channel walls and do not clog the channel. Indeed, the salt concentration at which each particle type ceases clogging is comparable to the Debye length at that concentration.

4.2 Remarks on Future Work

Our work in Chapter 2 reveals that a simple alteration in the shape of a channel has a large effect on the channel's clogging behavior. Understanding the clogging behavior of tapered channels can lead to improvements in microsieves and nozzles similar to nozzles used in inkjet printers. For example, the clogging of nozzles in devices like 3D printers may be delayed by widening the entrance of the nozzle. Moreover, our findings may also help predict clogging in more complicated systems such as blood vessels and porous media.

A logical next experiment is alteration in the particle's exit trajectory from the tapered channel. Our microchannels (in Chapter 2) tapers to a constriction that abruptly open into a wide area immediately after the constriction. Such a rapid change in geometry causes an abrupt decrease in the particle's velocity upon exiting the constriction. Our geometry change is much more abrupt in our channel arrays in Chapter 2 than in our single channel of Chapter 3. Understand the velocity decrease may offer insight into the channel array's clogging behavior and may also enable the clogging behaviors of single channels to be better understood in channel arrays. Future experiments may also test the influence of spatial variations in particle velocity immediately after the constriction. Specifically, increasing the ratio between a particle's speed in the constriction and the particle's speed immediately after exiting may allow particle to collide in the vicinity of the constriction even at low volume fractions. Increased particle collisions would dramatically alter the clogging behavior and may reveal

a new clogging mechanism.

In Chapter 3 we demonstrate clogging due to the detachment of clusters for the first time [*]. In regards to our specific experimentss, we suggest that future work focus on extracting even more quantitative data in relation clogging mechanisms. Specifically, particle velocity is likely connected to whether a channel clogs due to cluster detachment. We expect that a particle's velocity will play a critical role in determining whether a particle will adhere to the wall. Additionally, knowing more information about the local fluid velocity will enable more precise estimations of the near wall shear stress and even the drag force experienced by particles and particle clusters. We also suggest measuring the interaction between particles and between particles and channel walls. We expect a relationship between interaction strength and the clogging mechanism. Going further, we foresee the possibility of clogging phase diagram that connects the clogging time, clogging mechanism and salt concentration.

Due to the qualitative resemblance between cluster detachment and embolisms, we foresee potential experiments to model veins and arteries. If the elasticity and surface interaction of blood vessels can be successfully mimicked in in microchannels, then embolisms can also be mimicked using techniques similar to the methods used in this dissertation. Once the physical conditions that engender embolisms are known, it will also be possible to determine the conditions that will eliminate or prevent embolisms altogether.

Finally, we directly connect the clogging behavior to length of the stabilizing molecule on the particle's surface and to the amount of salt dissolved in the continuous phase of the suspension. Our results show an "on-off" switch for clogging. When the correct amount of salt is added, clogging ceases. One exciting prospect of this idea is the injection of brine into clogs that have already formed to destabilize the buildup and unclog. Another application of this knowledge lies in particle analysis

[*] At the time of publication, the authors were unable to find any other experiments showing clogging induced by detaching particle clusters.

and characterization. Given the observed ”on-off” behavior, it is feasible to devise a microfluidic chip that can cheaply estimate the length of stabilizing molecules on a particle' surface.

Rather than an exhaustive future research itinerary, the aforementioned projects represent just a few projects that immediately come to mind and are relevant to the work completed in this dissertation. Undoubtedly, there are many more investigations to be performed on this topic. Throughout the course of the experiments described in this dissertation, it became very clear that clogging is a fascinating, multifaceted enigma that will give decades of challenges and joy to the dedicated researcher who doggedly pursues her mysteries.

In an honest search for knowledge, you quite often have to abide by ignorance for an indefinite period.

Erwin Schrodinger

A

Negative Results and Experimental Advice

Publishing negative scientific results is a controversial issue[21,11,18,8], even though it is rarely it is rarely practiced. This dissertation is not going to make an argument in this debate except to state that negative results had a large impact on my work. I learned as much from experiments with negative results as I did from experiments whose outcomes are published. During the exploratory phase of my experiments, I learned more my negative results than from studying the literature. I reason that if I learned a great deal from my negative results, perhaps my reader can benefit in some way as well. In service of this cause, I have included a concise description of a couple experiments whose results were not included in the previous projects. Also in the spirit of helping other researchers, I have also included a short section on experimental tips and techniques that have served me well.

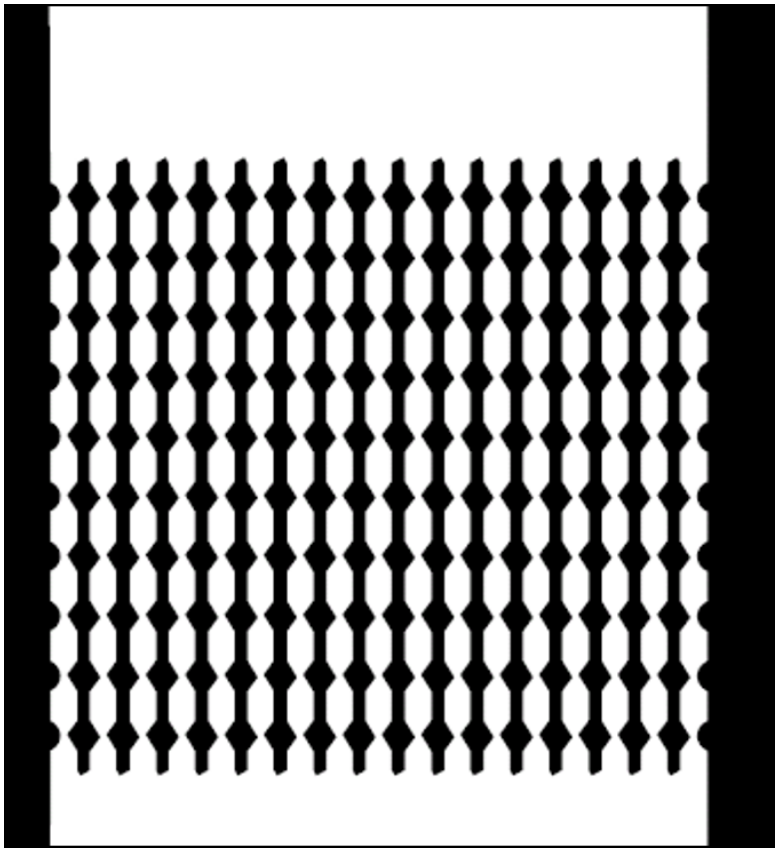

Figure A.1: Illustration of array of 16 channels whose width varies between 70 μm and 20 μm over a length of 1 mm. These channels are similar to the channels used in published clogging experiments.).

A.1 Clogging Periodically Varying Microchannels

Initially I sought to replicate the "bottleneck" design channels that were used in the previously published experiments[30] as shown in Figure A.1.

Similar to experiments in Chapter 2, we used pressure driven (2 PSI) flow to drive a suspension of 3 μm diameter polystyrene particles through the channel array. The particles were suspended at a volume fraction of 4% (w/v) and the particle surface was electrostatically stabilized with carboxyl groups. Using optical microscopy, we recorded the clogging experiments at 1 fps (Sony) and mea-

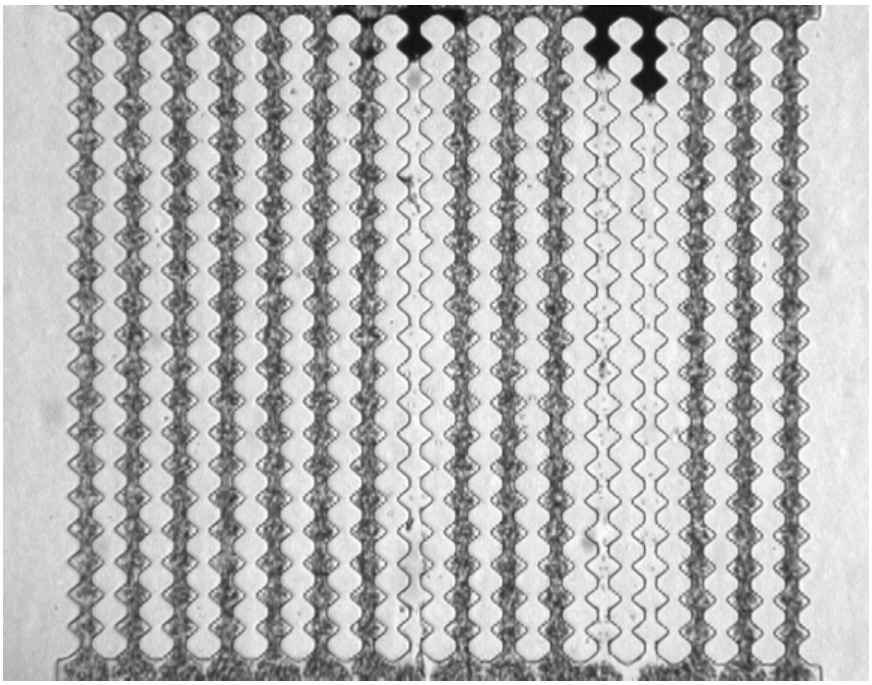

Figure A.2: Clogging experiment in progress using the bottleneck channel design.).

sured the time for each channel to clog (Figure A.2).

Using the time each channel takes to clog, we estimated the number of particles that pass through each channel before clogging the methods similar described in Chapter 2. On average, 4×10^7 particles pass before the first channel in the array clogs, an average of 6×10^7 particles pass before the second channel clogs and so on until all channels clog after an average of 10^9 particles pass through the channel array as shown in Figure A.3.

An average of 10^8 particles per channel pass before clogging (with an uncertainty of 40%). This number is nearly five times larger than the number of particles per channel reported to pass through before clogging in earlier published experiments.[30] This large difference in clogging behavior can be explained by differences in channel shape and particle type. Although we attempted to closely replicate the channel design published in previous experiments, our replications were not exact. Dif-

ferences between our replicated channels and the channels from published experiences may have contributed to the difference in clogging behavior. Additionally, published experiments used particles whose surface was stabilized with carboxyl and sulfate groups while our experiments used particles' surfaces were stabilized with only carboxyl groups. Therefore, a difference in surface interaction may have also contributed to the difference between our results and the previously published results.

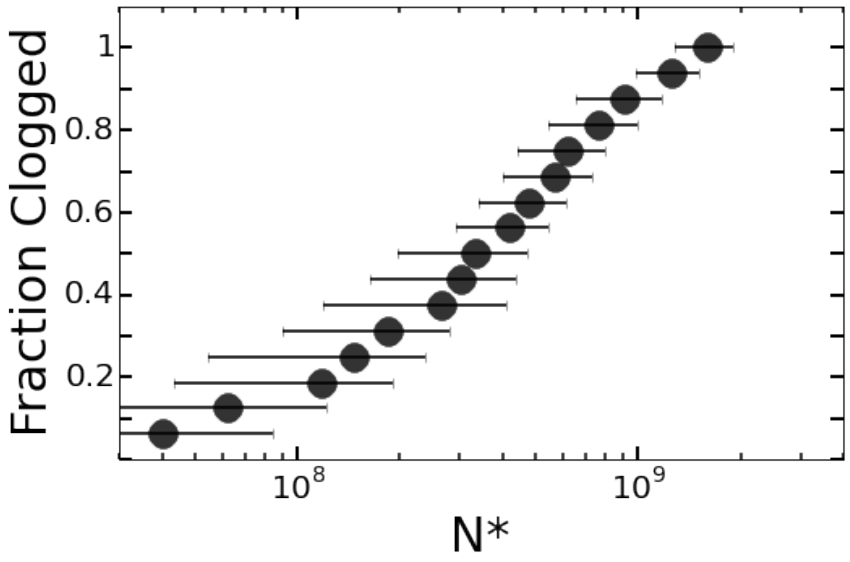

Figure A.3: Plot of Fraction Clogged vs. Time to Clog.

A.1.1 Multi-Channel Arrays

Using the bottleneck channel shape, we tested whether the number of channels in an array affects the clogging behavior. We clogged arrays of: 2 channels, 4 channels, 8 channels, 16 channels, 32 channels and 64 channels. As in previous experiments, we used $3\mu m$ diameter polystyrene particles suspended at 4% (w/v) in water. Again, we applied a pressure of 2 PSI to the particulate suspension and recorded the clogging behavior. We estimated the number of particles that passed before clogging by

collecting the suspension that exited the channel arrays and measuring the mass of the suspension. With the mass of the suspension, its density (approximately the density of water) and the particle number density, we estimated the total number of particles that passed through the array before completely clogging. The total number of particles that pass through the array prior to clogging increases linearly with the number of channels in the array as shown in Figure A.4. This linear relationship shows that the number of particles that pass through each channels is independent of the total number of channels in the array.

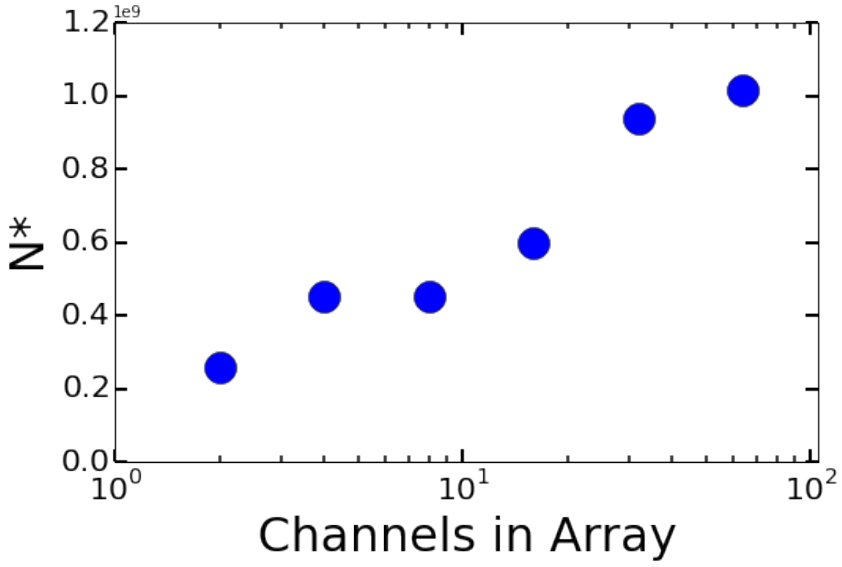

Figure A.4: Plot of N* vs. Number of Channels in the Array.

A.2 Experimental Tips and Warnings

During the initial stages of the work presented in this dissertation, I spent an inordinate amount worrying about dust in my experiments. In fact, my concern was so severe that it bordered on paranoia. Dust was of a great concern because if a single piece of dust entered the microfluidic channels, it would engender clogging. Any experiment with dust would be discarded because of the dust's

interference with the channels' clogging behavior. After spending a lot of time worrying, I realized two things about dust.

First, I learned that unfortunately dust cannot be completely eliminated in typical laboratory settings.* Dust is unavoidable. No matter how hard I tried there was always a piece of dust, a bit of dirt or even a tiny chip of PDMS that broke free from the channel wall. There was no way to avoid discarding microchannels or to avoid aborting experiments before completion. Fortunately, with PDMS based microfluidics it is easy to fabricate many arrays of microchannels or many single microchannels as once. I quickly became comfortable discarding microfluidic channel arrays if dust was present. Also, I gravitated towards shorter experiments. If dust interrupts a short experiment, little time and effort is sacrificed.

Second, I learned that the presence of dust could be minimized with a few simple habits and tools. First, I developed a habit of using lint-free wipes to clean any laboratory area prior to use. Additionally, I liberally used Scotch tape and Ziploc bags. The Scotch tape was very useful in removing dust from PDMS and other surfaces while the Ziploc bags provided a lint-free, airtight environment to store microfluidic chips. Also, even if all environmental dust is eliminated, PDMS chips and flakes can detach and clogg the channel. Many of the PDMS flakes orginated in the punched hole for the inlet and outlet tubings. To minimize PDMS flakes, we used sharp biopsy punches that cut more smoothly. Prior to rinsing with IPA, we applied compressed air to any punched hole in an attempt to detach any PDMS flakes. Even with these habits, I discarded many microfluidic channels and stopped many experiments due to the presence of dust.

As briefly mentioned in the Acknowledgments, my work in clogging began with yeast cells as a clogging agent. I strongly discourage anyone interested in clogging from using live cells, at least in initial work. The cells were polydisperse and their interaction with surfaces was difficult to control because

*A cleanroom is nearly free of dust. However, dust can also manifest from the particle suspension and chips of PDMS can break off in the channel. Therefore a clean room will not necessarily solve the dust problem.

cells of surface of cells are significantly more difficult to modify than colloidal particles. Additionally, cells must be grown in an incubator and inevitably a proportion of the cells die. Presumably dead cells have different properties from live cells and thus any experiments with cells are sensitive to the ever changing proportion of live cells to dead cells.

References

[1] (2015). *Handbook of Porous Media, Third Edition*. CRC Press.

[2] Bacchin, P., Derekx, Q., Veyret, D., Glucina, K., & Moulin, P. (2013). Clogging of microporous channels networks: role of connectivity and tortuosity. *Microfluidics and Nanofluidics*, 17(1), 85–96.

[3] Blankenhorn, D. (1989). Prevention or reversal of atherosclerosis: review of current evidence.

[4] de Jong, J., Lammertink, R. G. H., & Wessling, M. (2006). Membranes and microfluidics: a review. *Lab on a Chip*, 6(9), 1125–1139.

[5] Duffy, D. C., McDonald, J. C., Schueller, O. J. A., & Whitesides*, G. M. (1998). Rapid prototyping of microfluidic systems in poly(dimethylsiloxane). *Analytical Chemistry*, 70(23), 4974–4984.

[6] Eddings, M. A., Johnson, M. A., & Gale, B. K. (2008). Determining the optimal pdms–pdms bonding technique for microfluidic devices. *Journal of Micromechanics and Microengineering*, 18(6), 067001.

[7] Evans, D. F. & Wennerström, H. (1999). *The Colloidal Domain: Where Physics, Chemistry, Biology, and Technology Meet*. Wiley-VCH, 2 edition.

[8] Fanelli, D. (2010). Do pressures to publish increase scientists' bias? an empirical support from US states data.

[9] Gradoń, L. (2009). Resuspension of particles from surfaces: Technological, environmental and pharmaceutical aspects. *Advanced Powder Technology*, 20(1).

[10] Gudipaty, T., Stamm, M. T., Cheung, L. S. L., Jiang, L., & Zohar, Y. (2010). Cluster formation and growth in microchannel flow of dilute particle suspensions. *Microfluidics and Nanofluidics*, 10(3), 661–669.

[11] Gupta, N. & Stopfer, M. (2011). Negative results need airing too.

[12] Henry, C., Minier, J., & Lefèvre, G. (2012). Towards a description of particulate fouling: from single particle deposition to clogging. *Advances in colloid and interface science*, 185-186, 3476.

[13] Hermans, P. & Bredee, H. (1935). Zur kenntnis der filtrationsgesetze.

[14] Hermia, J. (1982). Constant pressure blocking filtration laws - application to power-law non-newtonian fluids.

[15] Israelachvili, J. (1992). *Intermolecular and Surface Forces: Revised Second Edition*. Intermolecular and Surface Forces. Elsevier Science.

[Kas] Kas, O. personal communication.

[17] M, S., T, A., & E, I. (1979). Blocking filtration laws for filtration of power-law non-Newtonian fluids.

[18] Matosin, N., Frank, E., Engel, M., & Lum, J. (2014). Negativity towards negative results: a discussion of the disconnect between scientific worth and scientific culture.

[19] Mirsaeedghazi, H. & Z, E. (2009). Changes in blocking mechanisms during membrane processing of pomegranate juice.

[20] Mustin, B. & Stoeber, B. (2010). Deposition of particles from polydisperse suspensions in microfluidic systems. *Microfluidics and Nanofluidics*, 9(4-5), 905–913.

[21] Ruben, A. (2012). Experimental error: I've got your impact factor right here. *Science*.

[22] S., K., I.W., H. R. C., & V.M., S. (2002). Modelling of dead-end microfiltration with pore blocking and cake formation.

[23] Sauret, A., Barney, E. C., Perro, A., Villermaux, E., Stone, H. A., & Dressaire, E. (2014). Clogging by sieving in microchannels: Application to the detection of contaminants in colloidal suspensions. *Applied Physics Letters*.

[24] Shaaban, A. & Duerinckx, A. (2000). Wall shear stress and early atherosclerosis: a review.

[25] Shun'ko, E. & Belkin, V. (2012). Treatment surfaces with atomic oxygen excited in dielectric barrier discharge plasma of o2 admixed to n2. *AIP Advances*, 2(2), 022157.

[26] Tegos, T., Kalodiki, E., Sabetai, M., & Nicolaides, A. (2001). The genesis of atherosclerosis and risk factors: a review.

[27] V.E., G. (1950). A critical investigation on the viscose filtration process.

[28] Wang, F. & Tarabara, V. V. (2008). Pore blocking mechanisms during early stages of membrane fouling by colloids. *Journal of Colloid and Interface Science*, 328(2), 464–469.

[29] Wennberg, O. P., Rennan, L., & Basquet, R. (2009). Computed tomography scan imaging of natural open fractures in a porous rock; geometry and fluid flow. *Geophysical Prospecting*, 57(2), 239–249.

[30] Wyss, H. M., Blair, D. L., Morris, J. F., Stone, H. A., & Weitz, D. A. (2006). Mechanism for clogging of microchannels. *Physical Review E*, 74(6).

[31] Yadeta, K. A. & Thomma, B. P. H. J. (2013). The xylem as battleground for plant hosts and vascular wilt pathogens. *Frontiers in Plant Science*, 4.